In the Name of Allah, the Most Compassionate, the Most Merciful

FILLER MATERIAL ESTIMATION FOR POTHOLES USING 3D PAVEMENT IMAGES

By

Syed Imran Moazzam Shah

2011-NUST-MS PHD- MTS-30

MS-70 (MTS)

Submitted to the Department of Mechatronics Engineering in fulfillment of the requirements for the degree of

MASTER OF SCIENCE

In

MECHATRONICS ENGINEERING

Thesis Supervisor

Dr. Khurram Kamal

College of Electrical & Mechanical Engineering

National University of Sciences & Technology

2013

DECLEARATION

I hereby declare that this thesis has been done by my own effort under supervision of Dr. Khurram Kamal. All the sources used for this work have been cited and the content has not been plagiarized. No portion of this thesis is submitted to any other degree requirement in any of the institutions.

_____

Syed Imran Moazzam Shah

ACKNOWLEDGEMENT

All praise is for ALLAH, the creator, the beneficent, the king and supreme in Greatness, to whom I trust and he shows me the way and Darood on Muhammad (p. b. u. h) and Ahl-o-bayt. Thanks to God for his supreme help in every moment of my life. I am grateful to my mother for her prayers, to father for his DNA and to my elder brother for his guardianship for a long time.

Many thanks to supervisor Dr. Khurram Kamal and co-supervisor Dr.Senthan Mathavan for their help and guidance and to the head of department Brig. Javaid Iqbal for his moral support and to other GEC committee members Dr. Kunwar Faraz Ahmed and Dr. Umer Shehbaz Khan for their valuable suggestions in the development of this quality work.

DEDICATION

To Mehdi (A.S.)

About whom the Holy Prophet has said,

"Even if the entire duration of the world's existence has already been exhausted and only one day is left before Doomsday (Day of judgment), Allah will expand that day to such a length of time, as to accommodate the kingdom of a person out of my Ahlul-Bayt who will be called by my name. He will then fill out the earth with peace and justice as it will have been full of injustice and tyranny before then."

Sahih Tirmidhi, V2, P86, V9, P74-75

ABSTRACT

Pavement distress and wear detection is of prime importance in transportation engineering. Due to degradation, potholes and different types of cracks are formed and they have to be detected and repaired in due course. Estimating the amount of filler material that is needed to fill a pothole is of great interest to prevent any shortage or excess, thereby wastage, of filler material that usually has to be transported from a different location. Metrological and visualization properties of a pothole play an important role in this regard. Using a low-cost Kinect sensor, the pavement depth images are collected from concrete and asphalt roads. Meshes are generated for better visualization of potholes. Area of pothole is analyzed with respect to depth. The approximate volume of pothole is calculated using trapezoidal rule on area-depth curves through pavement image analysis. In addition pothole area, length, and width are estimated. Accuracy of Kinect Sensor in data acquisition is addressed while imaging on water filled potholes to check its performance in rainy environment. Percentage errors are provided to have a comparison between actual and calculated measurements.

TABLE OF CONTENTS

LIST OF FIGURES

Figure **Page**

LIST OF TABLES

Table **Page**

1. INTRODUCTION

This chapter provides introduction about the problems created by pothole deformations in the pavement, research aims, motivation lying behind this research and brief description of methodology used to get to the results.

1.1. INTRODUCTION TO THE THESIS

Potholes are a significant feature of many parts of the highway network and are an irritation and nuisance to road users and highway maintenance staff alike. These localized failed areas also reduce ride quality and potentially create a dangerous driving condition. Various methods have been proposed so far, in order to detect pothole and also to characterize in terms of their shape, size, depth and volume. This is important to evaluate the extent of this distress, so that an appropriate maintenance measure can be taken. Some of the failed pavement areas are shown in Fig. 1.1.

Figure 1.1. Potholes in pavement

In addition to manual measurements, vibration sensing, image and video analysis, and laser based techniques have been employed in practice. Techniques such as taking manual measurements are labor intensive, less accurate and subjective processes. On the other hand, vehicle vibration based measurement is economical but again not capable of providing either any volumetric measurement. Laser based methods are precise but expensive in terms of hardware requirements, data storage and processing equipment. Machine and industrial vision cameras are expensive and require proper lighting arrangements. Moreover, stereo-vision that

is often proposed for 3D depth calculation has the disadvantage of its own that it cannot be used in Low light conditions and at night. However, the use of infrared technology based Kinect sensor for this purpose is a novel idea. Moreover, it is cost effective as compared to industrial cameras. The proposed method provides a low-cost alternative for the 3D analysis of pavement distress images. As compared to stereo-vision, in which 3D coordinates are calculated from two images, 3D imaging with Kinect sensor has the advantage that fewer calculations are required. As it provides direct depth measurements, therefore, need for computing power is drastically reduced. With Kinect, the night-time imaging can be done without any problem.

1.2. RESEARCH AIMS

The size and depth is an important factor to define the extent and severity of potholes. It is therefore important to measure the volume as accurately as possible. Manual survey is a slow process, labor intensive, and it is practically impossible to measure the volume due to the irregular shape of the pothole. The assessment could also be subjective as well as may create dangerous conditions for road inspectors, especially when the inspection is done after diverting traffic. Advancements in the field of image processing and machine-vision have added automation, removed the subjective element and improved the quality of road assessments when compared with manual surveys.

1.3. MOTIVATION

Increasing traffic volumes and heavier loads, allied with repeated adverse weather is causing significant deterioration in ageing road materials, resulting in millions of potholes and failed areas (cracking, localized depressions). These localized failed areas not only reduce ride quality, but potentially create dangerous driving conditions. Due to hazards caused by potholes to the public and economic set-back to the government, the subject has generated significant interest.

1.4. POTHOLES REPAIRING IMPORTANCE

Bad roads cause damage to vehicles, are annoying to drive on and sometimes these failed areas cause hazardous conditions to the drivers and pedestrians [1]. Harsh weather, heavy traffic loads and normal wear and tear are the sources which cause degradation to the roads in weeks to months. So, keeping the roads in good working condition is a challenging task [1].

Comprehensive and cheap pavement condition survey is essential to ensure good pavement condition at minimum investment [23]. Visual pavement assessment is a time-consuming and expensive procedure [24]. Potholes damage vehicles, cause irritation and accidents during swerving to avoid these failed areas. Due to these reasons South African government has launched a budget of 22 billion to repair the pothole in three years [25].

American of the United States travel approximately three trillion miles annually. American Society of Civil Engineers (ASCE) report card show evaluation grade D for American pavement infrastructure, which reports that the structure is close to failing [26]. For highway's condition improvement, a cost of $186 billion per year was estimated in 2009 in U.S. [26]. United States motorists are found to spend an extra vehicle repairs and operating costs of $67 billion a year for driving on their failed roads. Moreover, from 2005 to 2009, 198,546 people died in traffic fatalities, one-third of which are caused by bad road conditions [27].

1.5. METHODOLOGY

For analysis and evaluation, potholes were imaged using the Kinect sensor using the Open Kinect software in the Ubuntu Linux environment the metric (mm) depth images are used for further processing. Matlab is used as the processing environment.

Images are taken with Kinect sensor held approximately at 0.8 meters above the ground and imported into the Matlab environment for further processing. An extensive data processing algorithm is written in order to process and extract the metrological as well as characterization features of the pothole.

For area calculation of a pothole, depth images are converted to binary images for every millimeter increment in depth. For each step, a binary area is calculated using Matlab built in function that gives number of *on* pixels. Final area at certain depth is calculated by multiplying binary area at that depth level and area of one pixel in world coordinates at that particular depth. Pixel area at certain depth is calculated from pixel length and width by triangulation method by using the law of cosines and the field of view of Kinect. Area vs. depth curves are plotted to characterize potholes followed by the trapezoidal rule with unit spacing to calculate approximate volume. A test-rig is also constructed, on which artificial potholes of known dimensions are created, and then the manual and algorithmic calculations of the pothole parameters are compared to comment on accuracy achieved.

1.6. SUMMARY

The chapter describes that

- The potholes are a significant feature of many parts of the highway network and are an irritation and nuisance to road users.
- The size and depth is an important factor to define the extent and severity of potholes.
- The potholes not only reduce ride quality, but potentially create dangerous driving conditions.

2. LITERATURE REVIEW

This chapter presents the previous work done in the area of pavement pothole detection; different pothole detection and severity calculation algorithms are devised using different sensors, which are detailed in this chapter.

2.1. POTHOLE DETECTION USING ACCELEROMETERS

Eriksson et al. [1] have studied mobile sensing of roads to monitor and report any potholes. The proposed approach uses an accelerometer and a GPS device to detect and locate potholes respectively. The detections from accelerometer are fed to a central server in order to analyze and determine if the pothole that needs urgent repairing. The authors have named the work as Pothole Patrol, which consists of a group of vehicles on which sensors are mounted; the project also consists of a central server. Data is collected using a GPS device and an accelerometer. The detections are uploaded to the central server which keeps the record of the detection provided by the setup. The experimental setup consists of seven cars on which Soekris 4801 embedded computer is deployed, a Wi-Fi card is used for data transfer to a central server, a Sprint EVDO Rev Network card, a GPS device for location data of detected pothole, mounted on roofs of cars for clear sky visibility and a 3-axis accelerometer sensor for the detection of various anomalies. Linux is used as the operating system. Accelerometer provides the detections of the potholes but several other false positives are also detected by it like manholes, curbs, railroad crossing and expansion joints. Driving conditions like turning, swerving and sudden braking are also a cause of fluctuation in accelerometer readings thus creating a source of noise. Further processing is required to separate different detections. High pass filter is used to remove low frequency components like vehicular acceleration, turning, veering and braking as these driving conditions also create low frequency fluctuations in accelerometer readings. Accelerometer traces for smooth road, pothole, rail crossing and expansion joint are shown in Fig. 2.1.

Although the proposed technique discussed in [1] is simple and low cost sensor is used, but it has a drawback that this accelerometer based detection system only provides pothole detection when cars hit a pavement pothole and therefore there are much more chances to miss the pothole detection. In addition, the accelerometer outputs have a high number of false positives.

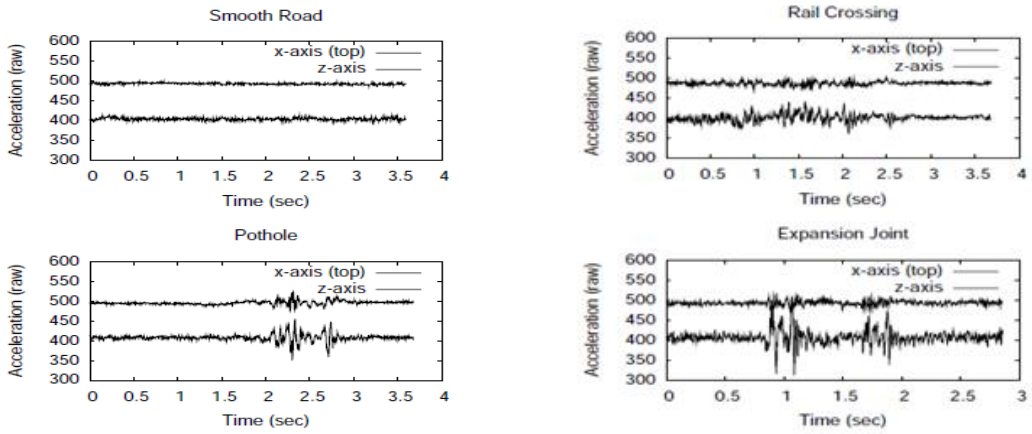

Figure 2.1. Accelerometer traces [1]

Aksamit et al. [2] have proposed a social distributed system using mobile phones equipped with a GPS and an accelerometer for pavement defects detection. In this work, a distributed network consisting of a number of mobile phones is used. An HTC Desire mobile phone is used to obtain data, the built-in accelerometer in mobile phones is used to get data according to surface roughness of the road. Detection of a pothole is done with greater accuracy, as accelerometer reading alteration becomes very high when a car hits a pothole. The system consists of a large number of mobile phones having built-in GPS and accelerometers, and is connected to a central server using internet GPRS connection to feed the data from the sensors. Accelerometer data acquisition, while placing mobile in pocket and on the dashboard of a car is shown in Fig. 2.2.

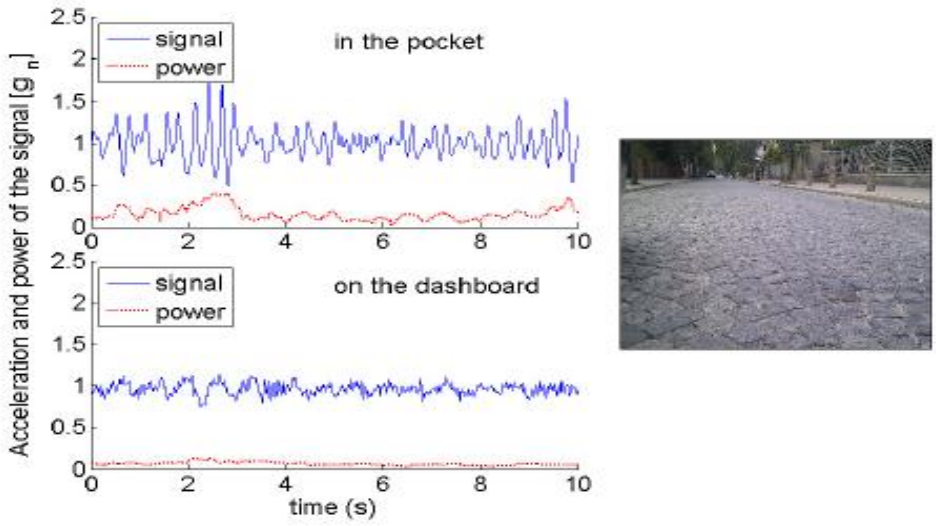

Figure 2.2. Accelerometer data acquisition [2]

For verification of results, 35 rides are done on same road with different combination of cars, mobile phones, and keeping the sensor at different places and accelerometer readings are collected each time. The system is able to detect and locate surface distresses. Accelerometer detects surface distresses but can miss detections when using for the purpose of pothole detection in case if image acquisition system does not hit the pothole, in which case there will be no change in accelerometer readings, which will result in no pothole detection.

2.2. POTHOLE DETECTION USING 2-D VISION

Koch et al. [3] have studied the vision tracking of potholes. The texture of potholes is compared with a reference texture of pavement. They have used a kernel based tracking of potholes. The pothole is detected first and then it is tracked. Matlab's image processing toolbox is utilized for data processing. This technique provides the number of potholes detected in a recorded video. Potholes are detected based on the fact that the texture of the pothole is coarser than the rest of the pavement surface. Firstly, thresholding is used and defect areas are separated from rest of the pavement. Then erosion is applied to approximate pothole, subsequently the pothole texture is cropped and compared with good conditioned pavement for cross check. A simple detection is shown in Fig. 2.3.

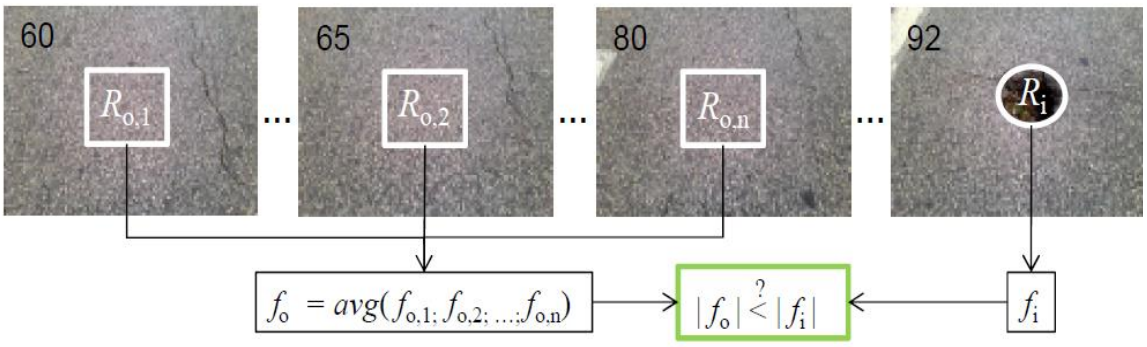

FIGURE 2.3. DETECTION PROCEDURE [3]

There are two advantages of this method; one is the reduced computational time as the algorithm uses pixels belonging to pothole instead of the whole image. Second advantage is that the algorithm texture comparison is less sensitive to changes in road appearance as it uses mean texture of pavement for comparison. Thirty nine pavement videos are collected with a remote controlled robot equipped with a webcam of resolution 640x480 having refresh rate of 30 Hz, installed at a height of 60 cm in downward direction. The algorithm uses 2-D

images, which lacks in depth data and so the algorithm is unable to provide information about the pothole's depth and volume.

Rajab et al. [4] have analyzed pavement potholes and evaluated their area through image processing. They have used curve fitting on edge points of pothole in 2D images. The paper reports the metrology of road cracks and potholes such as length, width and area. Manual measurements are also made in order to make comparison with the algorithm based measurements. They used ImageJ, which is an open-source image processing software. Fig. 2.4. shows the patch manual measurement and curve fitting on the same image.

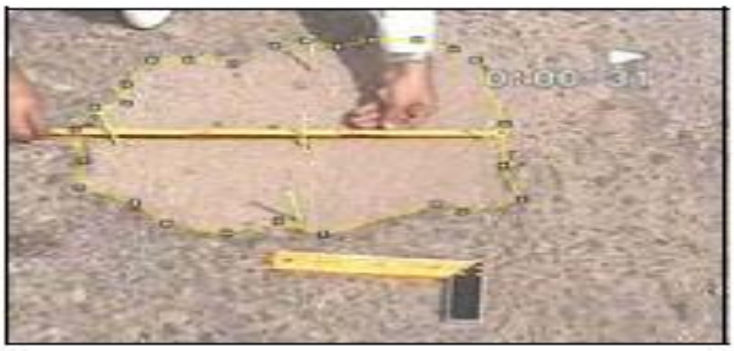

FIGURE 2.4. MANUAL MEASUREMENT AND CURVE FITTING [4]

Pothole area is calculated using curve fitting. Spline is fitted to the points at the boundary of the pothole, and the measured value of pothole is then compared with the corresponding manual measurement. 2D vision is used in this project using only one RGB camera, the technique is simple but lacks in depth calculations. The method cannot provide information related to pothole depth and volume.

Yao et al. [5] have applied the second order moment operator on pavement surface images and calculated the major axis, minor axis, and orientation of the potholes. The visual characteristics of defective and normal regions of road are different. When analyzing the values of an image, which has defective and non-defective regions, it is found that the non-defective region show more consistency on values as compared to the defective region. First order statistics such as, mean and variance are used to discriminate defective and non-defective road surfaces. To extract image features, second moment operator is used that is followed by a binary image conversion. Detected pothole by using binary image is shown in Fig. 2.5.

FIGURE 2.5. APPLICATION OF SECOND MOMENT OPERATOR FOLLOWED BY CONVERSION TO BINARY IMAGE [5]

The algorithm relies on 2-D vision using one camera and is much more sensitive to texture changes in pavement however, algorithm is unable to provide depth profile of the captured pavement surface.

Lin et al. [6] have proposed an idea for pavement pothole detection using support vector machines. It is observed from the potholes images that there is a granular section between pothole and its outer border. The granular section is extracted first to detect a pothole. Segmentation is done using partial differential equations in order to extract the object boundary and shape. From segmented images a granular section is detected to find the potholes. Eigenvalues of gray scale images are calculated and normalized between 1 to 10. Closed curves are then extracted, the region enclosed by these curves is declared as a pothole. The detection of a pothole is shown in Fig. 2.6.

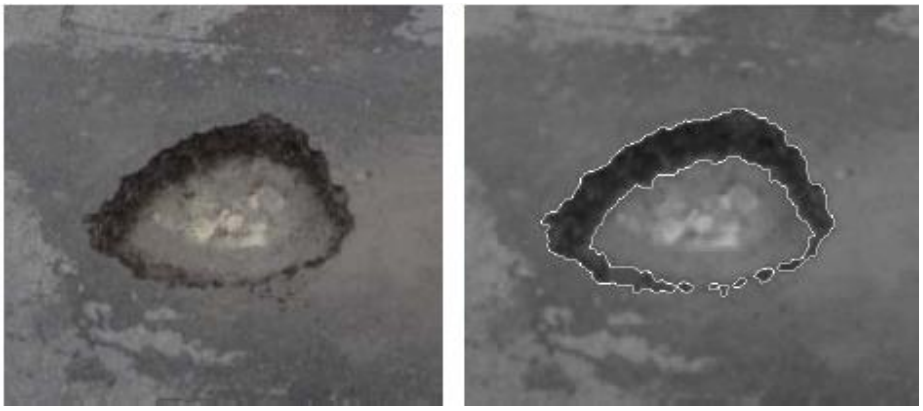

FIGURE 2.6. POTHOLE BEFORE AND AFTER DETECTION [6]

Salari et al. [7] have devised a genetic algorithm for pavement pothole detection. Extracting distress with threshoulding process from pavement is the major issue in pavement image

analysis. After the pavement images are captured, image segmentation is performed by applying an optimal threshold to extract pavement distress. A matrix of square tiles in generated on the distresses regions and then a three-layer feed-forward neural network is applied on the generated matrix for a type classification.

2.3. POTHOLE DETECTION USING STEREO VISION

Youquan et al. [8] have performed pothole detection using three dimensional projections. A line LED and two camera sensors are used. The LED band light show different behavior on the pothole with respect to the smooth surface. After initial processing and binarization, the pothole is detected efficiently. The whole system consists of a LED line light which is projected at road surface vertically. Two CCD cameras inclined at road surface at an angel between 30 to 60 on both sides of LED light. The experimental setup is shown in Fig. 2.7.

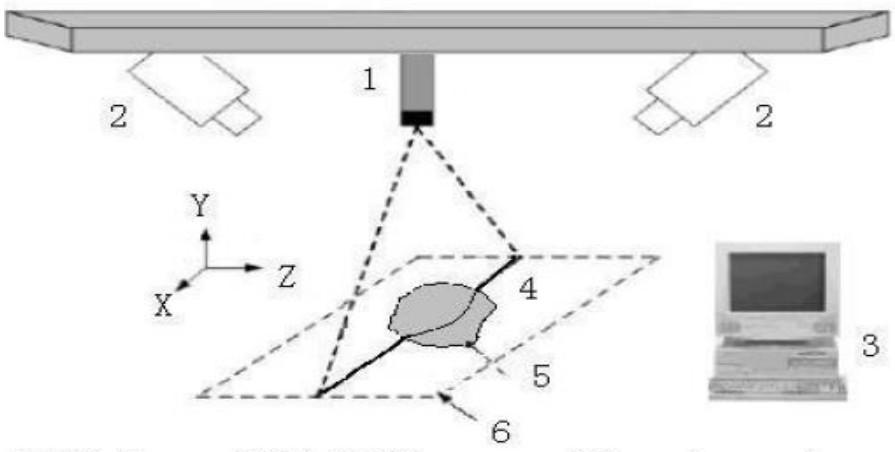

FIGURE 2.7. EXPERIMENTAL SETUP [8]

The LED band light does not show any variation at smooth surfaces but when it comes in contact with any depth variation then the LED light is deshaped. 3-D projection is used to calculate the actual coordinate values at the defect. Deshaping of the band light is shown in Fig. 2.8. The paper describes a technique which is a type of stereo vision, but the whole surface is not reconstructed, instead a band is analyzed to detect the pit damage on the road. The algorithm is efficient in finding potholes using stereo reconstruction but other information such as, pothole width, area, perimeter and volume cannot be calculated.

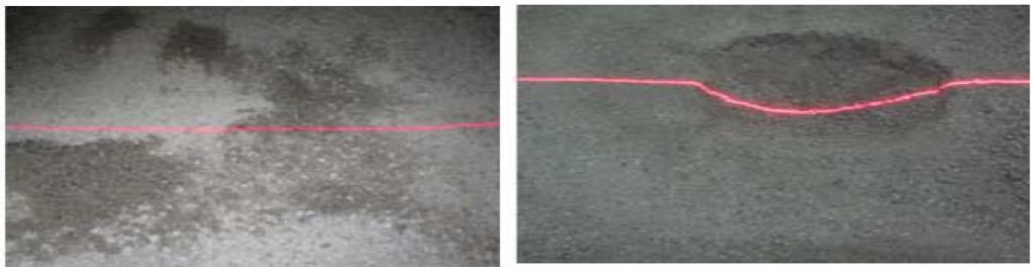

FIGURE 2.8. DESHAPING OF BAND LIGHT [8]

Stereo vision has been used by Salari et al.[9] for the detection and evaluation of pavement distresses. They have reconstructed the road surface and aimed to calculate severity of distress in future. Two cameras are used to take images of the same scene. From the two images taken same points are matched followed by a 3-D reconstruction. The technique has advantage that it cannot be confused with foreign objects such as, shadows, oil spills and tire marks. The process of 3-D reconstruction in shown in Fig. 2.9.

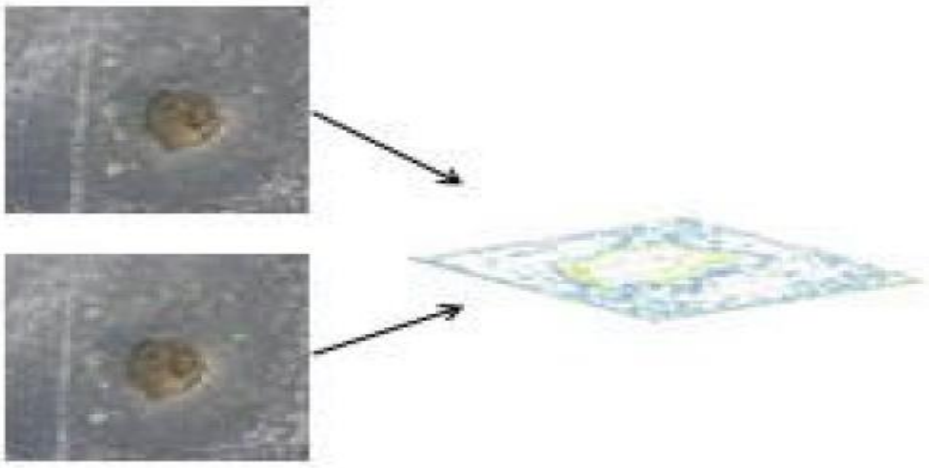

FIGURE 2.9. 3-D RECONSTRUCTION [9]

Wang et al. [10] have reviewed on automated pavement survey and proposed a stereo vision technique to get comprehensive information from 3-D modal of the pavement. 3-D surface reconstruction is done on acquired images taken with two cameras. The two images obtained are matched and depth information is calculated, 3-D model of pavement is then used to get surface conditions. The algorithm flow chart is shown in Fig. 2.10.

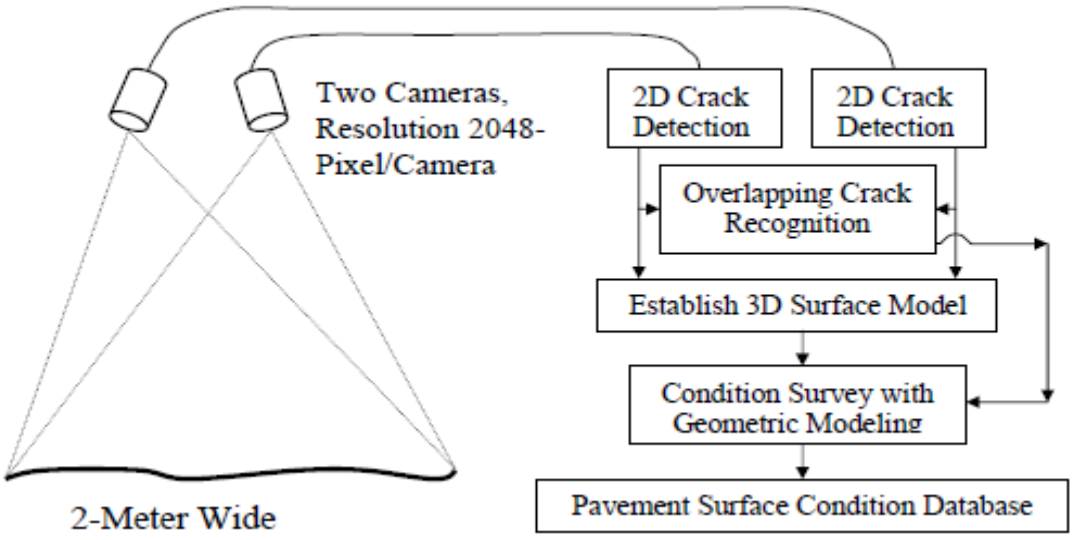

FIGURE 2.10. ALGORITHM FLOW CHART [10]

2.4. POTHOLE DETECTION USING LASERS

Yu et al. [11] have used laser images to detect and measure the pavement potholes. Laser line is projected on road. The laser line shows deformed pattern on potholes than on smooth surface. The shape of laser line provides the pothole information, which is extracted with further processing on resulting image. The experimental setup is shown in Fig. 2.11.

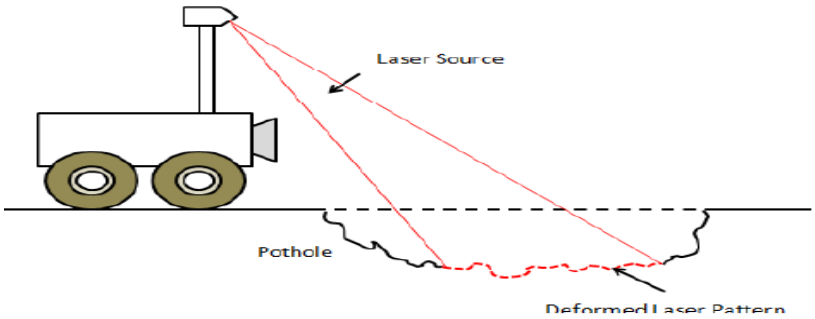

FIGURE 2.11. EXPERIMENTAL SETUP [11]

Impulse noise and noise due to external lighting are filtered out of the acquired images and processed to find laser line. Median filtering is initially used to remove the noise. For pothole feature extraction, the images are converted to binary images by taking suitable threshold. As laser source project a strong beam on road, so, the noises like lane marks, tire marks and oil spills create no effect on the image value. For automatic thresholding, the Otsu method is

used, pixels of gray scale image with values less than threshold are taken as distress pixel and the rest of the pixels are taken as background. Some of the results of this approach are shown in Fig. 2.12.

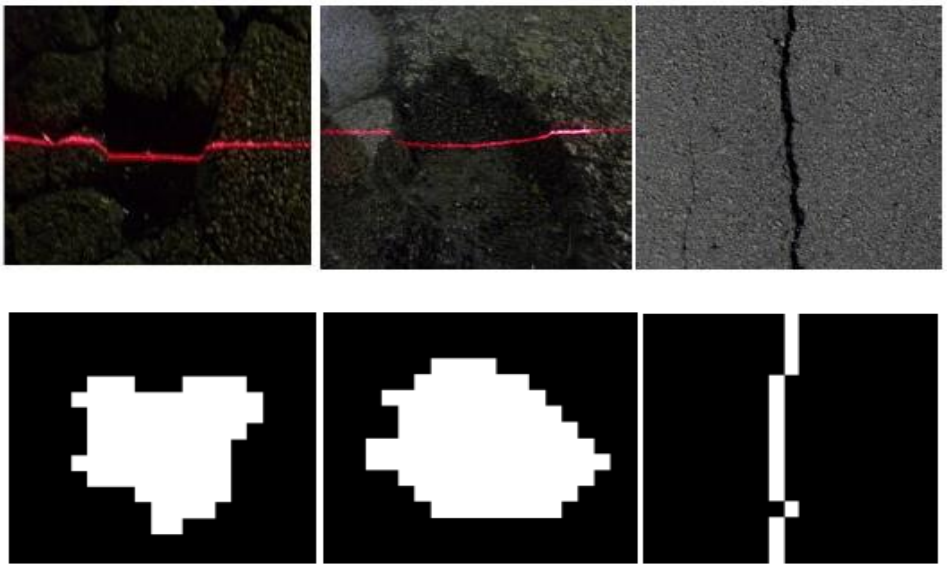

FIGURE 2.12. ROAD ROUGHNESS SCANNING AND BINARIZATION [11]

A template is generated for normal condition laser line and template matching is done to distinguish between potholes and smooth surfaces. Crack type and pothole severity is calculated using a three-layer feed forward neural network. The method is efficient in providing data information but the laser based system is power consuming and costly. The algorithm is designed to provide pavement deformation detection, not to compute depth information.

Sy et al. [12] have deployed a vision system for pavement surface crack detection. Imaging is done with two line scan cameras mounted on a vehicle at angel of 30 degree. The road surface is illuminated with two laser based illuminators to remove the effect of lighting conditions. The survey speed is maintained at 80 km/h. The imaging resolution is 1mm per pixel. Cracks are extracted based on the fact that they are usually darker than other road regions. A sample detection is shown in Fig. 2.13. To detect cracks, histogram equalization is applied to improve the contrast first followed by a bi-level threshoulding. And then morphological closing followed by a morphological opening is applied and at the end, result images are projected at four orientations at 0°, 45°, 90° and 135°.

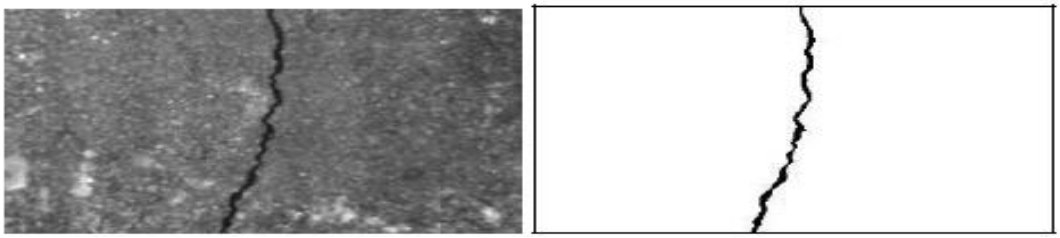

FIGURE 2.13. CRACK DETECTION [12]

The images with cracks show peaks when projected at these orientations, compared to others which have no defect. Laser illuminators are used for the purpose of removing lighting effects, not for obtaining and using 3-D information.

Laurent et al. [13] have utilized lasers to generate 3-D model of road surface to detect various pavement distresses. Two synchronized laser illuminators are used to obtain intensity 3-D profile of the road. In addition they also have devised an algorithm which detects and measure rutting and cracking. A video camera is used as a position detector and is mounted along z- axis. The laser scanners are able to obtain 1024 pixels per line and 300 profiles per second, 60 degree angle of view and operating distance of ½ meters. The projections mirrors are placed at 45 degrees, the scanner are kept 2 meters apart and 2.25 meters above the road surface in order to cover a road width of 4 meters. Road scan with this equipment is done at 100km/h to achieve the depth and intensity information. Vibration and shock tests are performed to evaluate the scanning accuracy. Rutting measurement is done through three steps. First of all, median filtering is applied to remove noise and artifacts due to pebbles and cracks in the road. The linear approximation is then done by fitting a line through first and last point of the pavement profile. Maximum distance between this fitted line and road surface is then calculated. On the basis of these three steps, the line is segmented into two if distance increases pre-defined threshold. This practice is repeated, which result in road profile approximation from which rut points are searched. From rut points, the depth of road rutting is approximated. Cracks are also detected using range images.

2.5. POTHOLE DETECTION WITH MISCELLANEOUS METHODS

Cafiso et al. [14] have employed digital techniques to acquire data from roads to save time and labor cost with a semi-automatic system. Images are collected with a high speed camera and are imported to the pavement distress analyzer software where optical noises are removed first. Then cracks, potholes and patching are detected automatically and classified with the assistance of an operator. A detection of pothole in pavement distress analyzer is shown in Fig. 2.14.

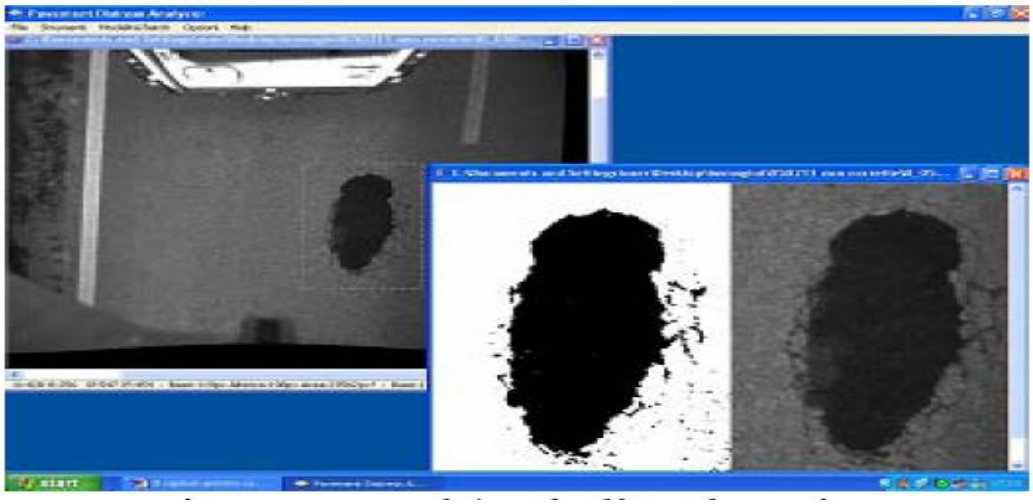

FIGURE 2.14. POTHOLE DETECTION [14]

Image data of pavement is collected with a digital camera mounted on mobile laboratory. The CMOS sensor has a resolution of 1288x1032 pixels and operates on frequency of 9.3 fps. After image acquisition, data is supplied to software where images optical distortion is removed and then pavement distress is extracted using thresholding. The data analyzer setup provides 2-D data and hence 3-D information cannot be measured.

Li et al. [15] have studied the backscatter response on road surface faults and stones at road at frequencies in millimeters. Radar is utilized to detect cracks and potholes in the pavement. The deformations in road such as cracks and potholes have unique backscatter response, from which these failed areas are detected.

Wei et al. [16] have applied wavelet theory and presented a pavement roughness analysis. He used frequency range from 0 to 3.28 cycles per minute to examine features of defected pavement at high as well as at low frequencies. Wavelet transform is used to calculate surface roughness.

2.6. KINECT SENSOR APPLICATIONS IN OTHER RESEARCH AREAS

Rakprayoon et al. [18] have studied Kinect sensor for its application in obstacle detection for robotic manipulators. Kinect sensor acquires depth data and the proposed algorithm is used to distinguish between manipulator and obstacles in the work space. The method of least square is used for calibration. OpenGL is used to generate 3D model of manipulator. The RGB image and its corresponding depth profile are shown in Fig. 2.15.

FIGURE 2.15. MANIPULATOR RGB AND DEPTH IMAGES [18]

Correa et al. [19] have utilized Kinect sensor in robotic navigation in indoor environment. The proposed system consists of two parts, first part consists of navigation algorithm for obstacle avoidance. The second part consists of an artificial neural network, which is used to get movement configurations. The system is not light dependent. Depth information from strips shown in Fig. 2.16 is used to decide a turn of mobile robot.

2.7. POTHOLE DETECTION USING KINECT SENSOR

Joubert et al. [21] have deployed a GPS, Kinect, and a USB camera for pothole localization and data collection. The GPS is used to locate the potholes. Pothole width is calculated manually using Kinect images and edges of potholes are detected from camera video sequence.

RGB image Depth image

FIGURE 2.16. KINECT'S RGB AND DEPTH VIEWS [19]

The system records 3-D point cloud data and location of detected potholes, the data is analyzed and processed to get the width and depth of pothole. The system is designed to get survey recordings at 60km/h. The sensor rack consists of a high speed USB camera and Kinect sensor, the recordings are done inside the vehicle where an onboard computer is deployed to keep the record, GPS is also attached to the computer. ROS is used as operating system, it has driver for Kinect sensor and data transfer structure, also it has OpenCV and PCL integrated on it. The paper presents its earlier manual results of pothole width and depth. Pothole manual width and depth calculations are shown in Fig. 2.17. The algorithm lacks in automated method to achieve goals like calculation of pothole length width, depth and volume.

FIGURE 2.17. POTHOLE MANUAL WIDTH AND DEPTH MEASUREMENT [21]

Jahanshahi et al. [22] have employed Kinect sensor for autonomous pavement defect detection. The pothole image and its mesh are shown in Fig. 2.18. Depth images from sensor are used to detect defects in pavement. A plane surface is fitted using RANSAC (Random Sample Consensus) on depth images first, and then depth image is subtracted from the fitted plane as shown in Fig. 2.19. Otsu thresholding method is used to discriminate between defected and smooth areas of road. Regions with at least 10mm depth are taken as on pixels in binary images. The pixel size taken is 1.38 mm, considering Kinect installation height of 77.8 cm.

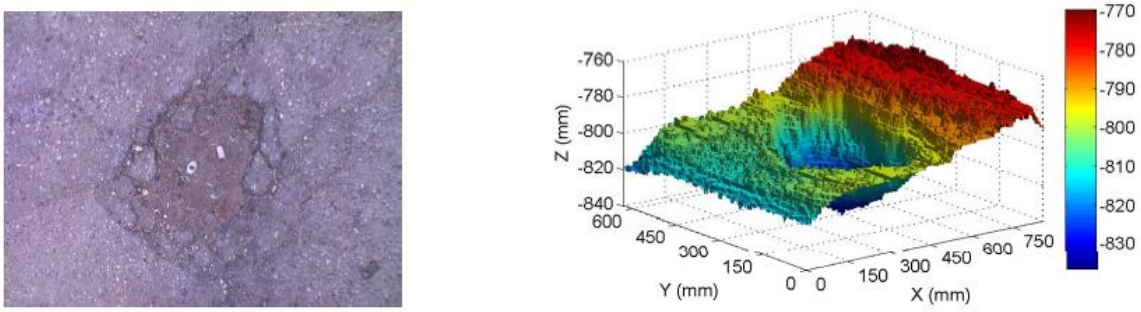

FIGURE 2.18. POTHOLE RGB AND MESH IMAGES [22]

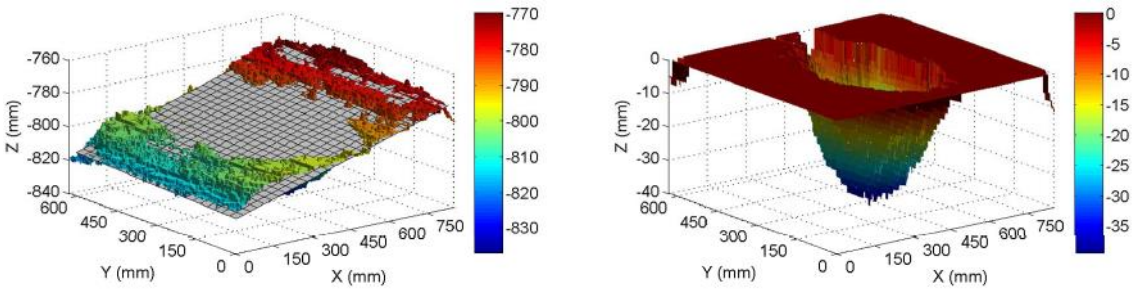

FIGURE 2.19. PLANE FITTING AND SUBTRACTION [22]

Rectangles are fitted to detected defects in images in order to calculate length and width of pothole as shown in Fig. 2.20. A GPS is used to localize the defects on map. At 77.8 cm height the Kinect field of view is reported to be 830 x 650 square millimeters.

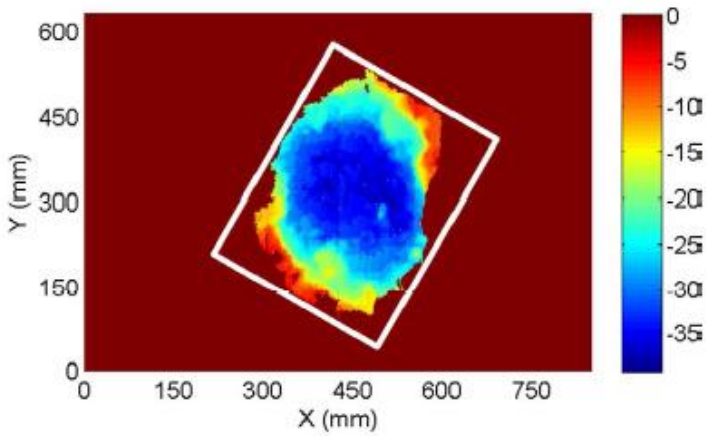

FIGURE 2.20. RECTANGLE FITTING [22]

The algorithm provides results validations in case of pothole length, width and depth but not in the case of volume. The method lacks in giving information about the depth profile and surface roughness. The algorithm utilizes RANSAC algorithm for plane fitting, which is affected due to the pothole, as the outliers cause erroneous plane fitting, thus the pothole extraction is not effective, hence the pothole parametric calculations are effected. The research does not provide any benchmarking process for pothole volume calculation, which is necessary for filler material estimation for pothole for pavement repair.

Table 2.1 shows a brief comparison between the various data acquisition techniques and their advantages and disadvantages.

2.8. SURVEY TECHNIQUES

TABLE 2.1. SENSORS COMPARISON

Techniques	Pros.	Cons.
Accelerometer	❖ Small storage ❖ Cost effective	❖ Wrong results ❖ Unwanted Detections ❖ Missed Detections
Vision	❖ Provide detections ❖ Pothole span can be calculated	❖ Depth is unknown ❖ Partial Detections ❖ Effected by Shading, Oil Spills
Stereo vision	❖ More accurate measurements ❖ Depth can be calculated	❖ Bad 3D Reconstruction accuracy ❖ High computational effort ❖ High storage
Lasers	❖ Accurate depth measurements	❖ High initial costs ❖ Significant power consumption ❖ Frequent maintenance
Kinect	❖ Less computational effort ❖ Less storage ❖ Low cost, Less power hungry ❖ Accurate as LASERs	❖ Infrared Interference while Direct Sunlight

2.9. KINECT SENSOR

Kinect for X-box is basically designed for gaming to remove the need of controller but later on researchers found its capability and potential in research so later on Kinect for window was designed for application development. However, both sensors can be used in research Kinect for Xbox through its various hacks like Open Kinect in Ubuntu Linux environment. Kinect for

Windows can be used directly in windows through its dedicated software or using Matlab to achieve its RGB and depth Images like simple USB camera.

Cruz et al. [17] have surveyed the Kinect sensor and its application in robotics, games, and in natural environments, etc., and conveyed important information about it. The IR camera operates at 30 Hz, the images are 640 x 480 pixel wide, can also be operated with 1280 x 1024 at 10 fps. Field of view is 58 degree horizontal, 45 degree vertical and 70 degree diagonal, the operation range is 0.8 to 4 meters, 2.6 to 11 ft. It also has a tilt motor, an accelerometer and microphones.

In order to get proper depth images, it is necessary stay away 0.8 meters. Both depth and RGB images have noise in them that can be reduced with average, Gaussian, or median filter. The sensor has potential to reveal the information about pavement and can be used as low cost solution, in pavement surveys.

El-Iaithy et al. [20] have utilized Microsoft Kinect in manipulators in shape detection from RGB camera and depth measurement from infrared projector and camera. The sensor has two modes of operations, default mode with blind spot from 0 to 80 cm and near mode with 0 to 40 cm blind spot. In indoor environment Kinect depth accuracy is as much higher as a laser with tolerance of plus or minus 1 cm as well as in outdoor environment avoiding direct sunlight accuracy remains same. Glass and transparent plastics are not detected by Kinect due to refraction. The sensor does not work in direct sunlight, so for pavement surveys, there is need of a canopy to shade the examined pavement surface. At night the sensor gives detections without any problem.

Kinect for Xbox and Windows are shown in Fig. 2.21.

FIGURE 2.21. KINECT SENSOR

2.10. SUMMARY

The chapter describes that

- The accelerometers are utilized in pavement pothole detection but unwanted detections and sometimes missed detections are the main problems of the sensor.
- The 2-D vision is most widely deployed to detect pothole but the sensor is unable to provide depth information of the pothole.
- The depth information can be calculated using stereo-vision but there 3-D reconstruction accuracy is limited.
- The LASERs provide accurate depth measurements but the equipment is costly and power hungry.
- The Microsoft Kinect sensor show good promise in pavement pothole detection and evaluation, it is low cost solution and provides accurate depth information.

3. METHODOLOGY

This chapter sets out the methodology of the research and elaborates how 3-D images are captured, imported into MATLAB's environment and processing steps in order to obtain various information about pothole like its length, width, area and volume.

3.1. PROPOSED TECHNIQUE

Images are captured with the Kinect sensor held approximately at 0.8 meters above the ground, facing towards pavement surface nearly vertical. Subsequently these images are imported into the Matlab environment for further processing. An extensive data processing algorithm is developed in order to process and extract the metrological measurements like pothole's perimeter, depth and volume etc. as well as characterization features which classify the pothole based on its 3-D geometry.

The metric depth images are captured using Openkinect software under Ubuntu Linux environment. Subsequently these images are imported in Matlab and are read as gray scale images ranging from 0 to 2^{16} using Matlab unit16 (16 bit unsigned integer) class. These images show variation in intensity of gray level from 0 which represents the zero depth and is shown by a black pixel to 2^{16} representing full depth shown by a white pixel. More white areas in the depth images show more depth in short. After the images are imported into the Matlab, unit16 data type is converted to the double data type, in which all the depth values are normalized between 0 to 1, and meshes of the potholes are generated.

A slight disorientation of the sensor creates a tilt in depth values. The tilt introduced in the depth values must be removed in order to correctly evaluate pothole parameters. To remove the tilt, a plane is fitted to the image depth values, and then the fitted plane is subtracted from the tilt image to achieve a tilt-less image. Then the tilt-less image is processed to get different parameters like major axis, minor axis and volume etc. of the pothole.

For volume calculation of the pothole, depth images are converted into binary images for every millimeter increment of depth. For each step, numbers of white pixels in the binary images are calculated. Area at a certain depth is calculated by multiplying number of white pixels at that depth level by the area of one pixel in world coordinates at that particular depth.

After areas at all depths are calculated, Area vs. depth curves are plotted, which show pothole area decay profile. The summation of area under these curves is volume, which is calculated

by applying the trapezoidal rule. For benchmarking to see error between manual and automatic measurements acquired by applying proposed algorithm, a test-rig is designed. Pothole classification is also done by analyzing its area decrease with respect to increase in its depth. Flowchart of the developed algorithm is shown in Fig. 3.1.

3.2. GRAPHICAL REPRESENTATION OF PROPOSED TECHNIQUE

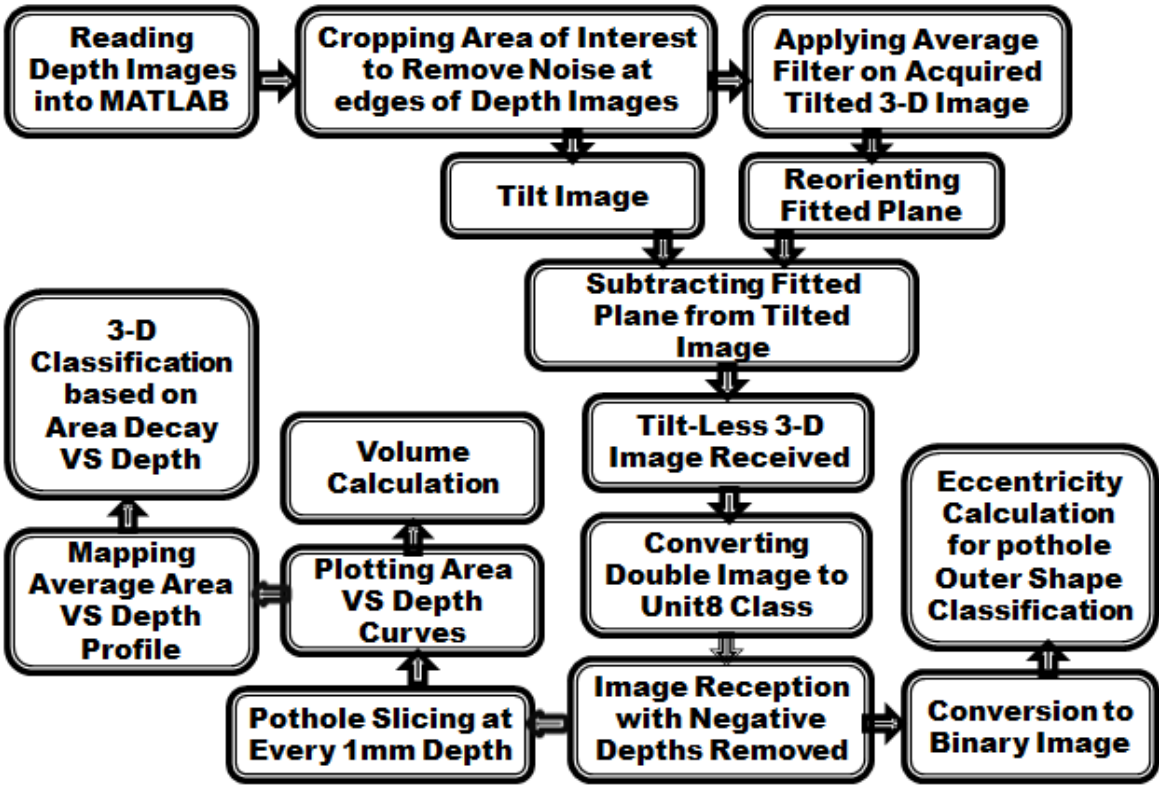

Figure 3.1. Algorithm flow chart

3.3. SUMMARY

This chapter details that

- The depth images are taken with the Kinect sensor held approximately at 0.8 meters above the pavement.
- The unit16 data type of images is converted to the double data type and meshes of the potholes are generated.

- For volume calculation of pothole, depth images are converted into binary images for every millimeter increment of depth and pothole areas are calculated.
- The area vs. depth curves are plotted to characterize potholes followed by the trapezoidal rule to calculate an approximate volume of pothole.

4. INITIAL EXPERIMENTATION

This chapter explains the experimental setup that is used to acquire 3-D pavement images. It also shows mesh results of the potholes generated by algorithm to provide better visualization. Area depth curves are generated to show pothole decay profile. It also lists out various metrological features of the pothole calculated by the developed algorithm.

4.1. EXPERIMENTATION

For analysis and evaluation, potholes are imaged in the NUST College of E&ME Rawalpindi, Pakistan, using the Kinect sensor. Image acquisition is performed using Open Kinect software under Ubuntu Linux environment. The metric (millimeter) depth images are used for further processing. Matlab is utilized as the image processing environment. The experimental setup deployed to acquire depth images is shown in Fig. 4.1.

Figure 4.1. Experimental Setup

Image on the left in Fig. 4.2 shows a depth image captured with the help of Microsoft Kinect sensor. A depth image from a Kinect sensor is a two-dimensional array of pixels and each location of pixel (x, y) stores depth values in millimeters sensed by the IR sensor. All the values of depth image provide distances in millimeters at each pixel. Higher values at pixels represent deeper points into the pavement surface.

Image on the right in Fig. 4.2 shows the corresponding RGB image of the same pothole acquired from the RGB camera of the Kinect sensor.

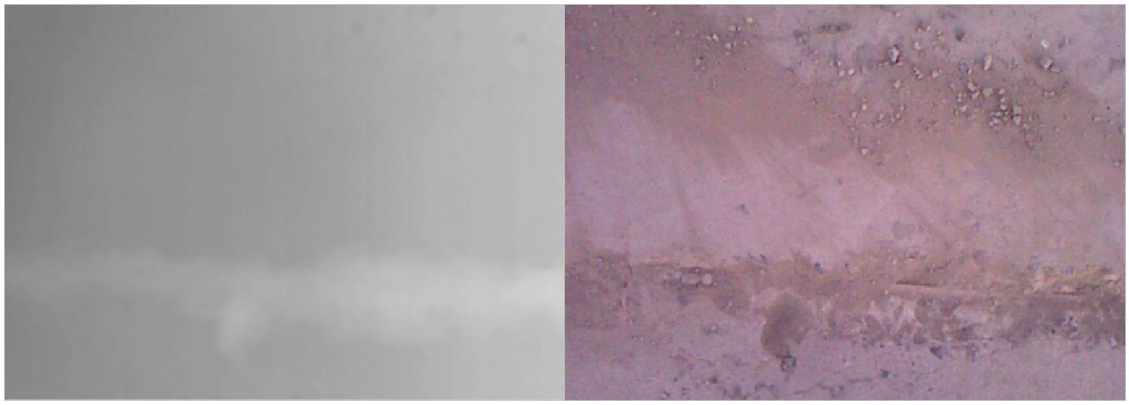

Depth Image RGB Image

Figure 4.2. Millimeter depthand RGB Imagesof a pothole through Kinect Sensor.

4.2. IMPLEMENTATION OF PROPOSED ALGORITHM

Fig. 4.3 shows a 3D plot of the pothole, with real-world coordinates given in millimeters. The potholes are shown upside down, greater depths are the points with higher peaks in the plot and meshes.

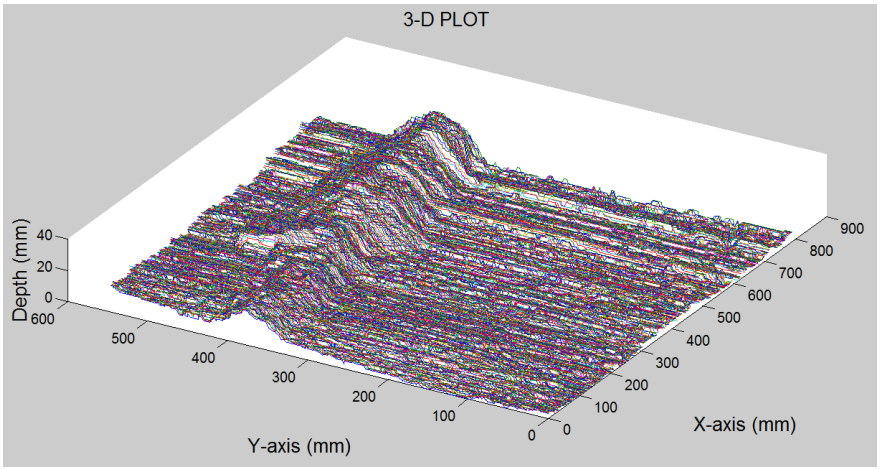

Figure 4.3. 3-D Plot result of the pothole

For better visualization, mesh plots with normalized depths are generated. The x and y coordinates of meshes are in real world coordinates (mm) while the z or depth axis is showing normalized real world double precision values from 0 to 1. The corresponding mesh and contour plot of the pothole are shown in Fig. 4.4. In contour plots dark red are the deepest points while dark blue are least deep.

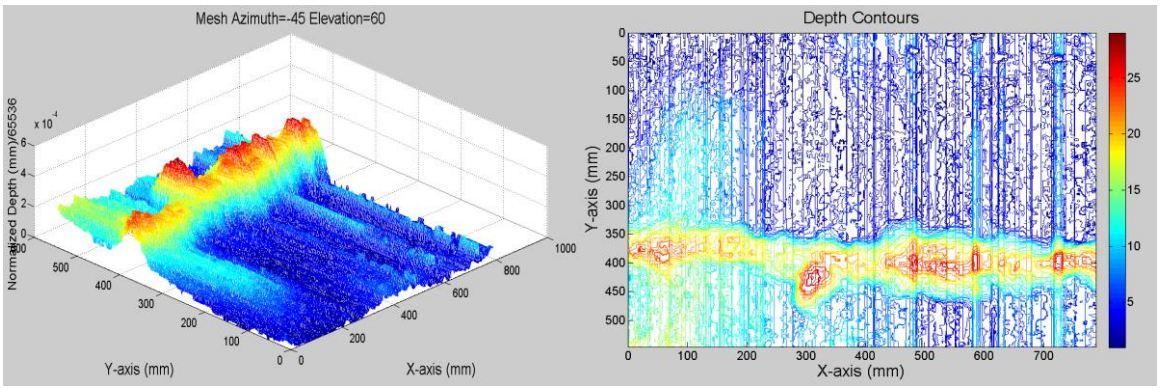

Mesh plot Contours plot

Figure 4.4. Mesh and contour plot of the pothole

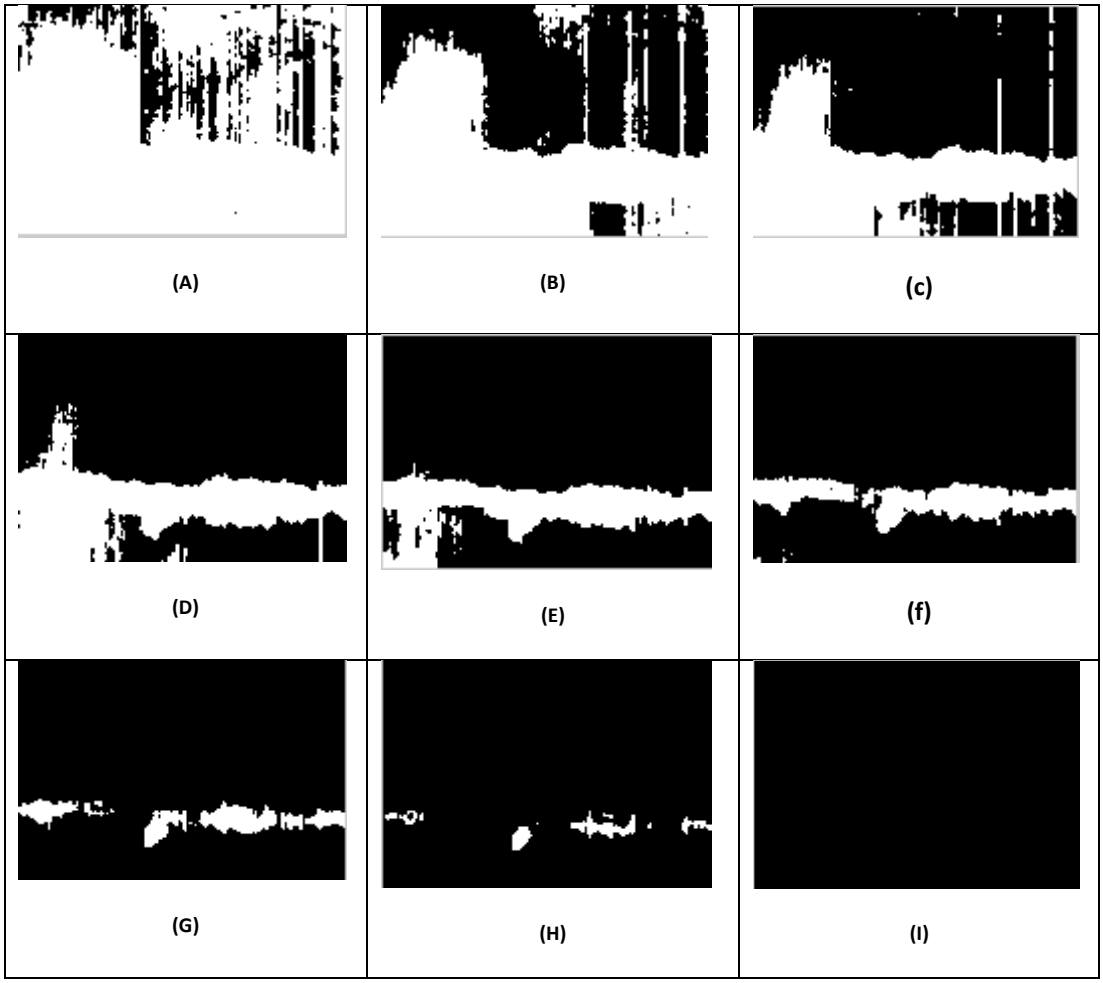

Figure 4.5. Binary Images of Pothole at 1,4,7,10,13,16,19,22 and 25 millimeters depth respectively.

Binary images are used to calculate areas at all depths. The *on* or white pixels show the depth of the pothole below certain depth as shown in Fig. 4.5. Fig. 4.6 shows the area verses depth plot. It shows how the area of the pothole is changing with depth. Eight different potholes are

selected for results and analysis and mesh details are shown in Fig. 4.7. Red areas belong to potholes while the blue areas correspond to pavement surface. The meshes show different profile as the size and shape of those potholes vary with respect to depth. (c) is longitudinal pothole, (d) is very big pothole nearly covering the whole imaging area while (b) and (h) are nearly circular potholes as shown by Fig. 4.7.

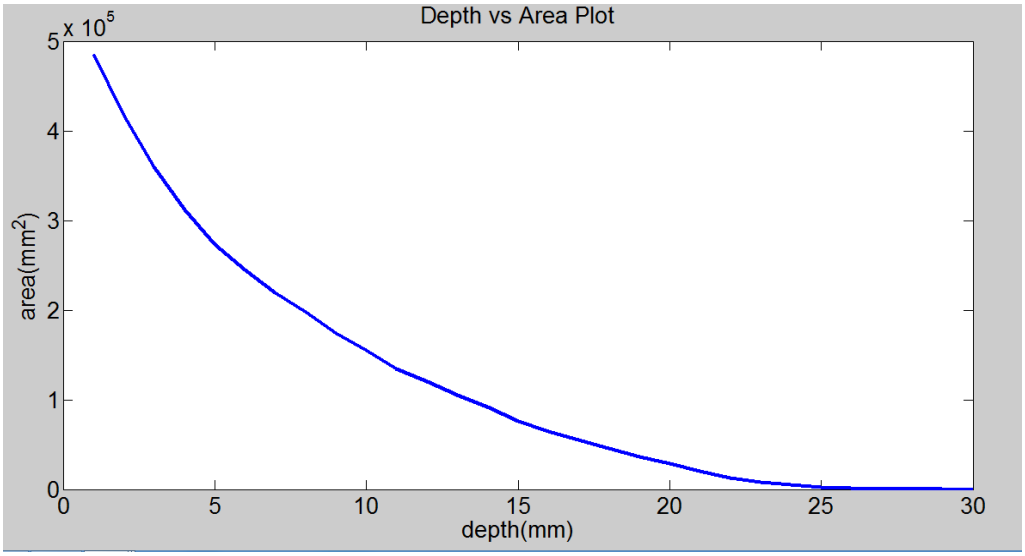

Figure 4.6. Plot of decay of Area with respect to Depth.

The plot of area decay with respect to depth provides some properties of potholes (Fig. 4.8). The end of each curve on x or depth axis tells that how much deep is that pothole. A prominent feature of the curves is that they all are monotonically decreasing.

Table 4.1 lists out some of the metrological parameters of the 8 potholes shown in Fig. 4.7. Approximate volume is calculated by applying trapezoidal rule on the area-depth curves (Fig. 4.8). The trapezoidal rule is given by equation 4.1.

$$\int_a^b f(x)dx \approx (b-a)\frac{f(a)-f(b)}{2} \qquad [4.1]$$

The pothole boundary is detected from binary images and region properties are calculated. These properties provide different metrological parameters of pothole like major axis and minor axis, centroid, eccentricity, orientation and perimeter, as listed in Table. 2. Major and minor axes provide the geometrical feature of pothole which convey an idea about the approximate length and width of the pothole respectively.

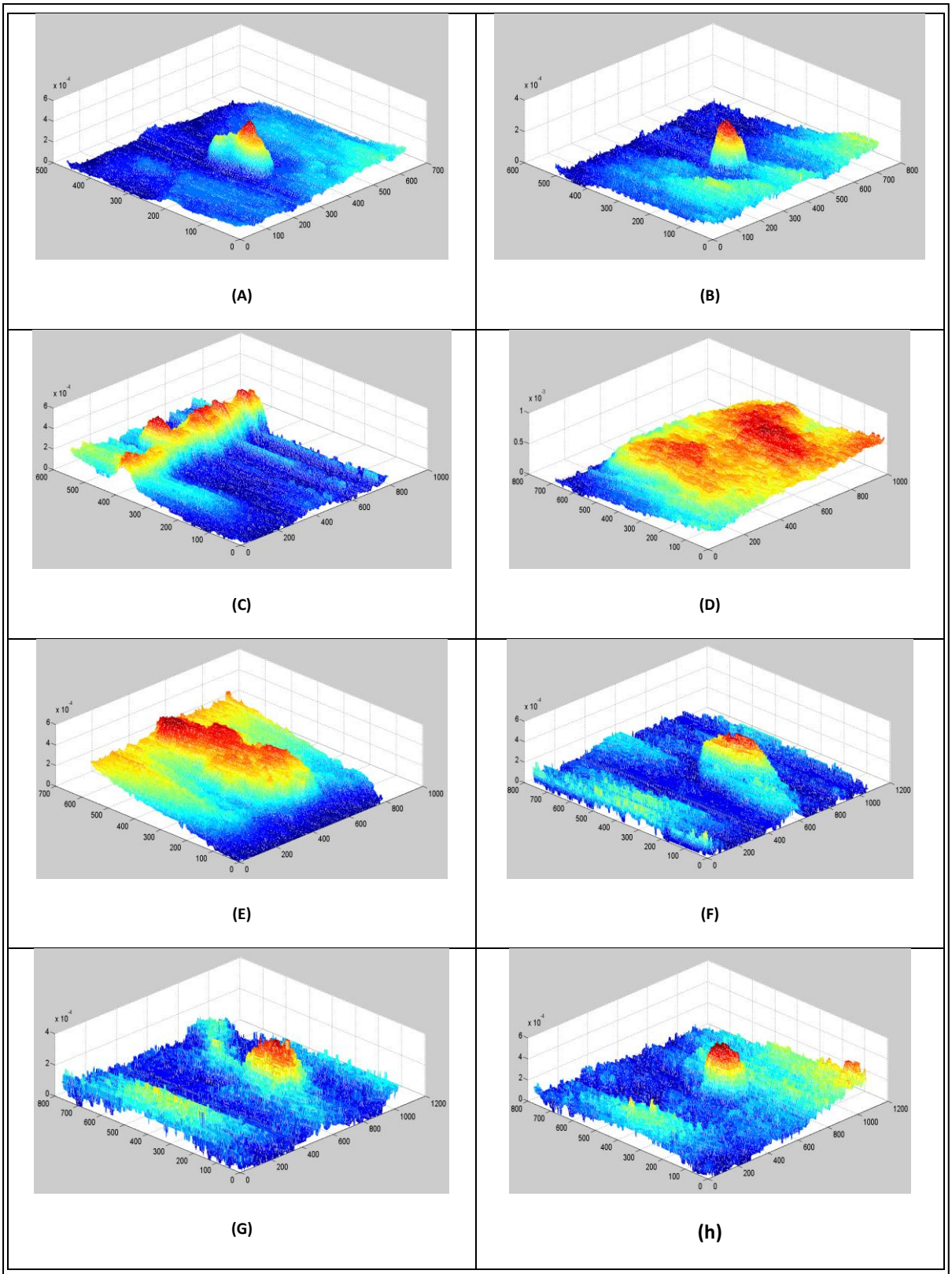

Figure 4.7. Mesh results of the potholes

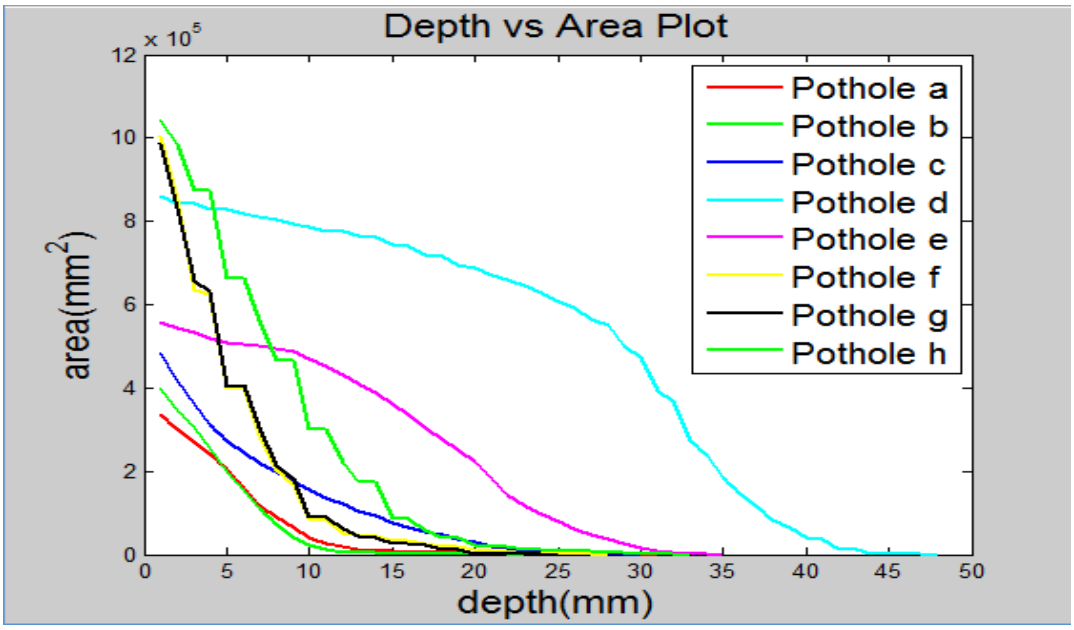

Figure 4.8. Plots of Area decay of all potholes with respect to Depth.

Table 4.1. Pothole Feature Table

Pot-hole	Max. Depth (mm)	Approx. Volume (cm^3)	Major Axis Length (mm)	Minor Axis Length (mm)	Centroid in x (mm)	Centroid in y (mm)	Eccentricity	Orientation (degree)	Perimeter (mm)
a	31	1760	182.45	112.60	375.40	248.72	0.78	-81.04	420.91
b	23	1742	95.92	83.34	368.64	213.76	0.49	50.72	251.76
c	30	3405	850.44	185.15	290.17	390.59	0.97	2.89	2705.1
d	48	23030	658.72	458.18	432.21	204.95	0.71	5.61	3298.1
e	35	9095	424.42	300.35	436.40	347.09	0.70	-83.10	2475.1
f	28	4543	167.19	105.19	507.67	236.23	0.77	86.49	686.90
g	25	4549	144.87	118.46	473.98	197.29	0.57	-35.39	711.83
h	33	7693	165.96	126.82	478.10	239.98	0.64	-19.7	1051.6

Centroid provides the information regarding the geometrical center of the pothole. The eccentricity is again a geometrical descriptor that provides the information regarding the shape of the pothole. For a perfectly circular geometry, the value of eccentricity should be zero; however, the potholes with eccentricity values closer to zero are circular, whereas for potholes having eccentricity values closer to one are longitudinal or elliptical in shape. The

orientation provides the measure of tilt of the major axis of pothole, in degrees, with respect to x-axis, and can have a value between -90 to 90.

4.3. SUMMARY

This chapter details that

- The image acquisition is done using the OpenKinect software in the Ubuntu Linux environment.
- All the values of depth image give distances in millimeters at each pixel.
- For better visualization mesh plots with normalized depth are generated.
- Approximate volume is calculated by applying trapezoidal rule on the area-depth curves.

5. TEST-RIG DEVELOPMENT & BENCH MARKING

This chapter describes the test-rig, which is designed for the purpose of benchmarking error calculation.

5.1. TEST-RIG DEVELOPMENT

A test-rig is constructed and designed for the purpose of comparison between manual and algorithm based measurement to comment on error rate. Concrete test-rig contains six artificial potholes of different shapes and dimensions. Different views of the drawing of the test-rig are shown in Fig. 5.1. The 3-D model of the test-rig designed using ANSYS Workbench is shown in Fig. 5.2.

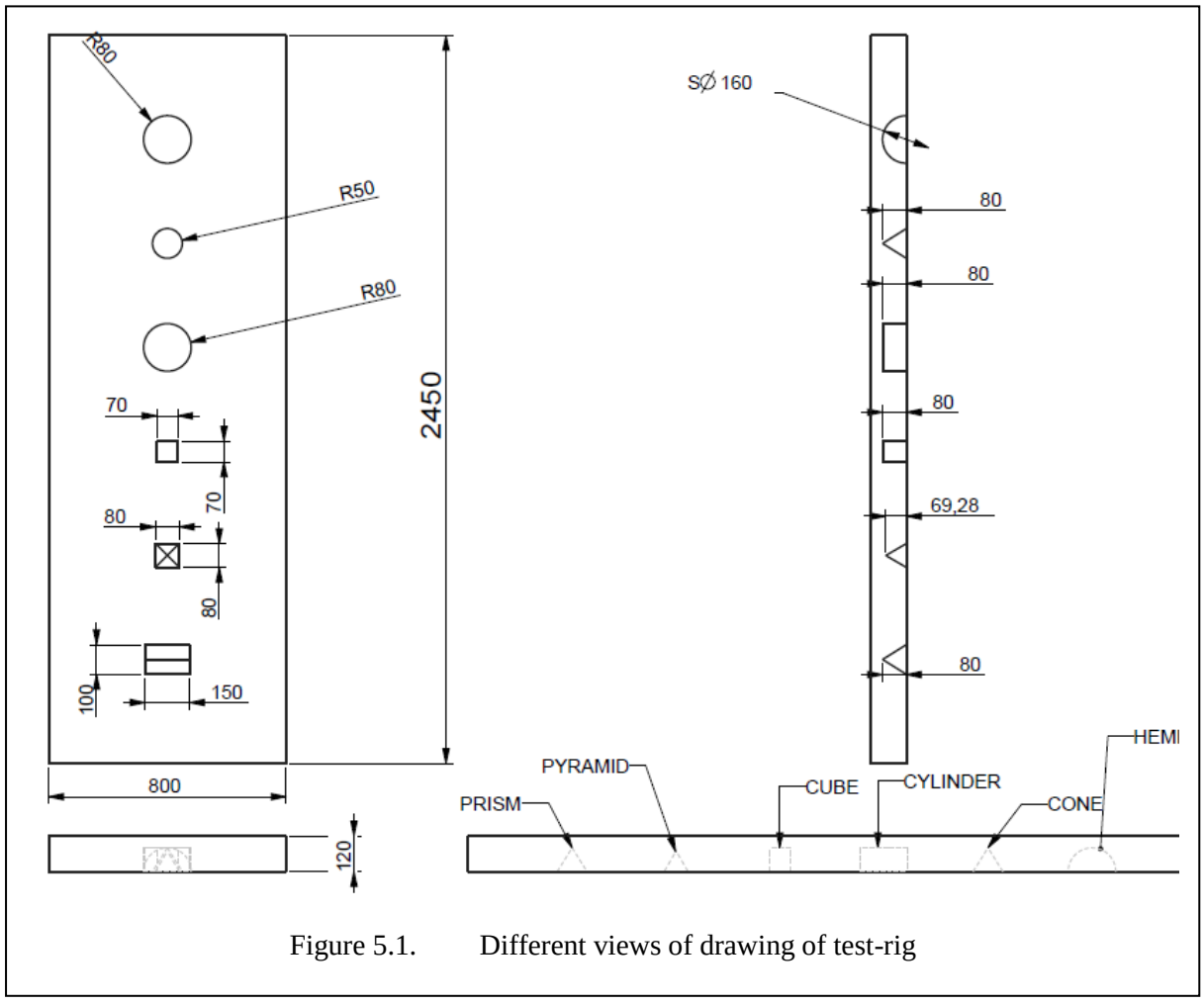

Figure 5.1. Different views of drawing of test-rig

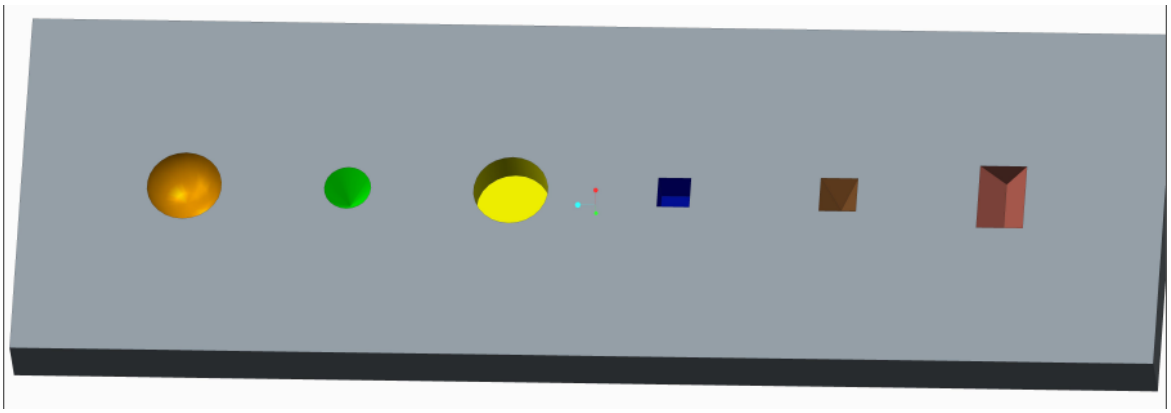

Figure 5.2. 3-D model of test-rig

Test-rig after construction is shown in Fig. 5.3.

Figure 5.3. Constructed Test-rig

5.2. ALGORITHM IMPLEMENTATION ON TEST-RIG

Metric depth and RGB images of a pyramid shaped pothole are shown in Fig. 5.4. The mesh of the pothole is generated and is shown in Fig. 5.5. The mesh is slightly tilt because of sensor disorientation. To remove the introduced tilt by sensor disorientation, fitted plane is obtained and shown in Fig. 5.6. The tilt is removed from image by subtracting fitted plane from tilted image as shown in Fig. 5.7. The mesh is shown complemented in Fig. 5.8.

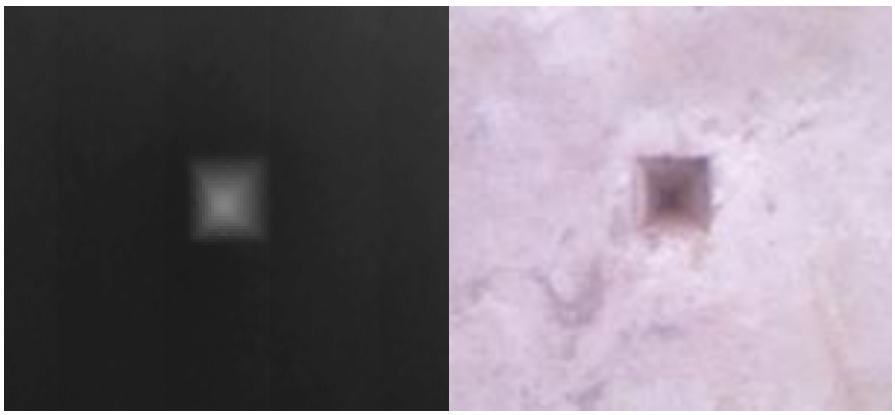

Depth image RGB image

Figure 5.4. Metric depth and RGB images of a pyramid shaped pothole

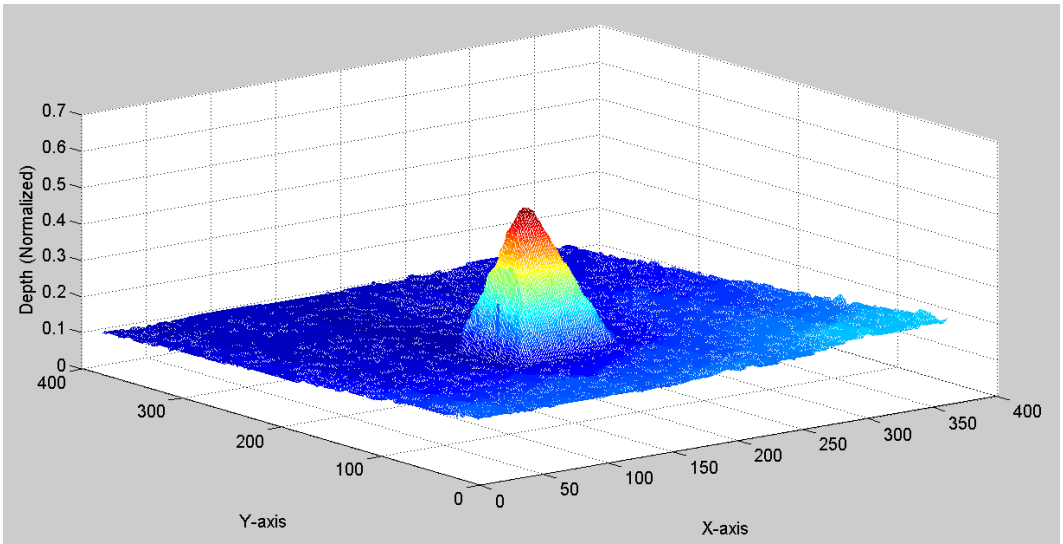

Figure 5.5. Mesh result of pyramid shaped pothole

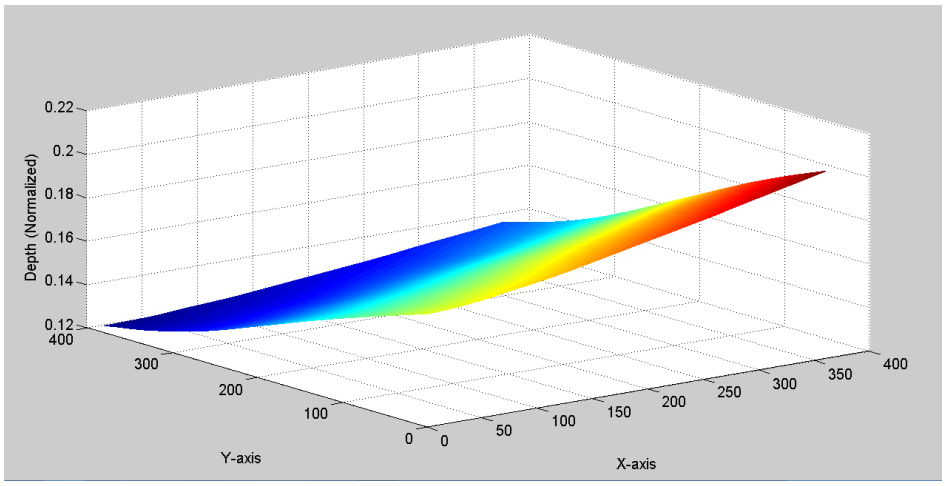

Figure 5.6. Mesh result of fitted plane

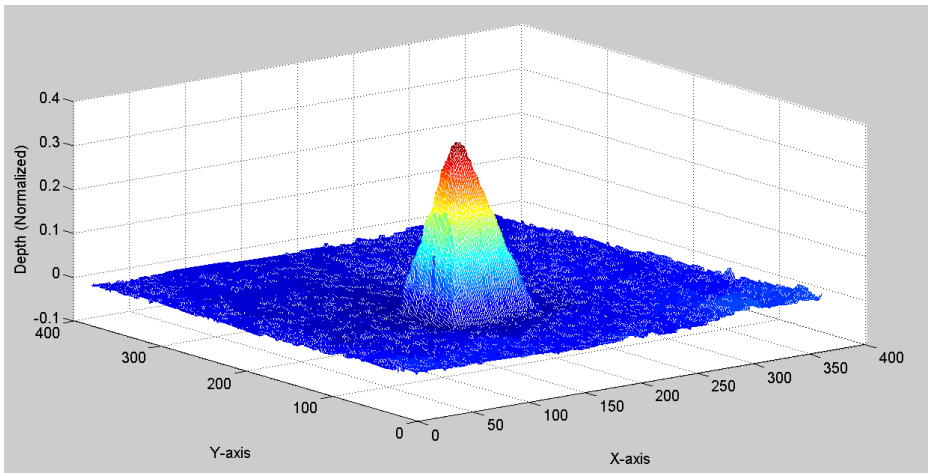

Figure 5.7. Mesh after subtracting fitted plane from the tilted image.

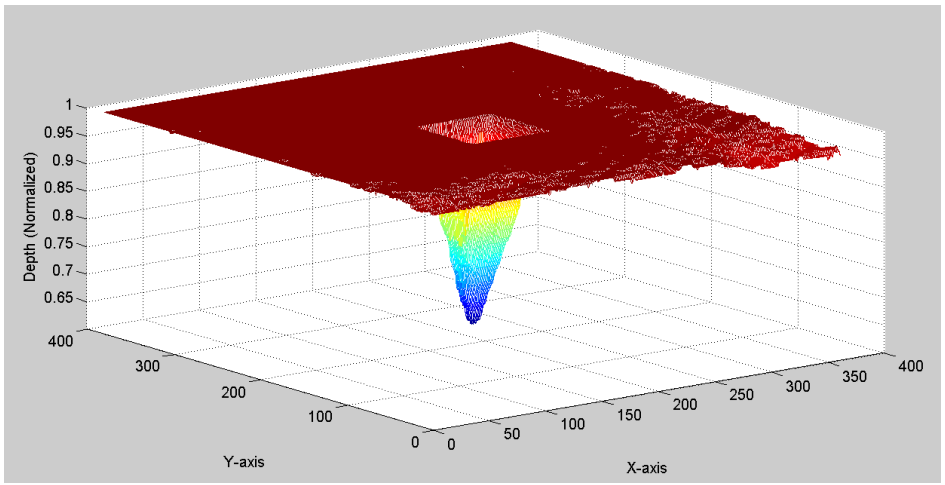

Figure 5.8. Complemented mesh

Figure 5.9 shows processed meshes of all six potholes of hemisphere, prism, pyramid, cone, cylinder and cube shapes created in the test-rig for algorithm performance analysis.

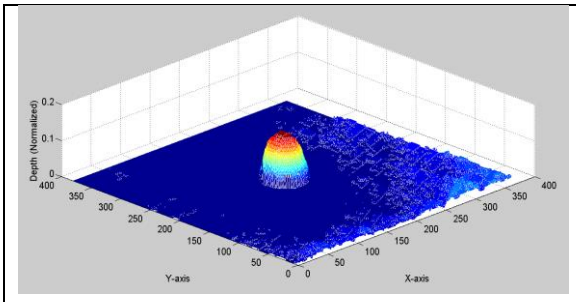

Hemisphere

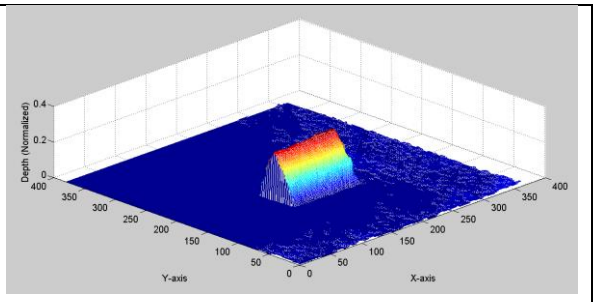

Prism

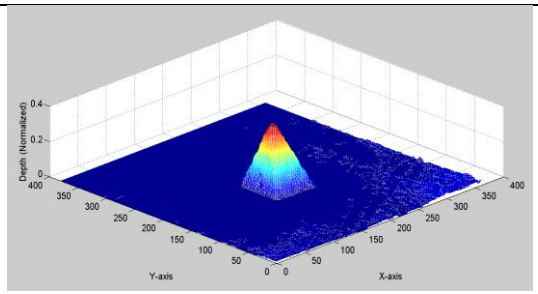

Pyramid

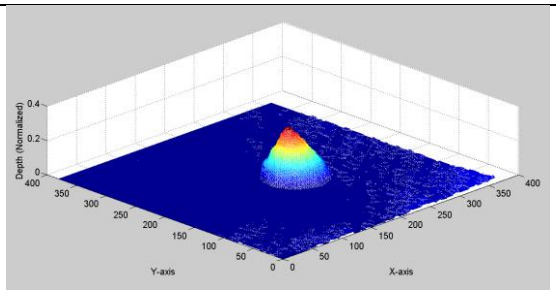

Cone

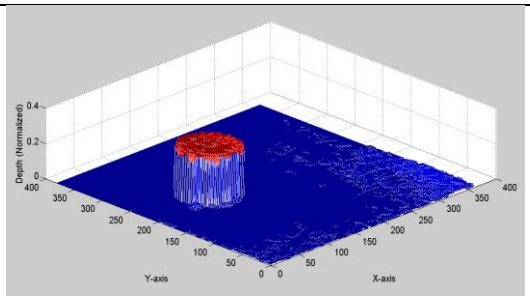

Cylinder

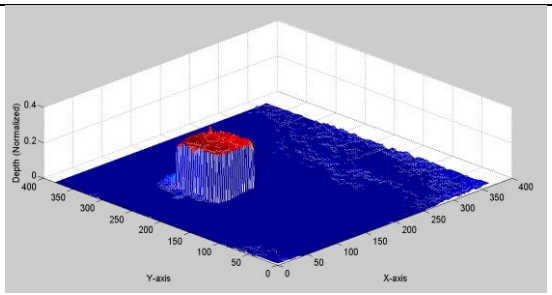

Cube

Figure 5.9. Meshes of test-rig potholes

Maximum depths of all potholes are calculated manually first, and then are subsequently calculated from depth images using the algorithm and percentage error is calculated. The comparison between manual measurements and measurements by using algorithm is listed in table 5.1. Similarly percentage error in volumetric calculations is listed in table 5.2.

Table 5.1. Pothole maximum depth table

Pothole	Maximum depth (mm)		
	Actual	Calculated	Error (%)
Hemisphere	40	41	2.5
Prism	78	81	3.8
Pyramid	100	97	-3.0
Cone	81	82	1.2
Cylinder	80	82	2.5
Cube	78	80	2.5

Mean Percentage Error (MPE) = 2.58 %

Table 5.2. Pothole Volume Table

Pothole	Volume (cm^3)		
	Actual	Calculated	Error(%)
Hemisphere	150	144	4.0
Prism	545	582	6.8
Pyramid	340	320	5.9
Cone	403	433	7.4
Cylinder	950	875	7.9
Cube	780	773	0.8

Mean Percentage Error (MPE) = 5.47 %

5.3. POTHOLE CLASSIFICATION

Two types of pothole classification are performed. The first is a 2-D classification which describe about the outer shape of the pothole and is decided by pothole's eccentricity value,

which is calculated from the pothole's binary Image. Eccentricity is the ratio of distance between the foci of the ellipse and the major axis length of the potholes. The ratio returns a value between 0 and 1. An eccentricity value of zero describes a circular porthole while longitudinal potholes are represented by a value of one. A 3-D classification, on the other hand, provides information about the pothole area change with respect to its depth. The decay of the particular pothole area provides information about its severity. The pothole mean area is calculated and a mean line is drawn with the area-depth curve of the pothole. Three types of potholes are classified with respect to mean area value. The area depth curves intersect with the mean line at different locations based on the pothole geometry. The four time area decay potholes (FTADPs) are fastest areas decaying potholes and there is a depth curve intersects with the mean line below 60 percent of depth values. The two time area decay potholes (TTADPs) are relatively slow decaying pothole and their area is a depth curve intersection with mean line between 60 to 80 percent of depth values. Non-Decaying potholes (NDPs) on the other hand, are much resistive to area decay and there area depth curve does not intersect with the mean line below 80 percent of the depth values. Depth vs. Area curves intersecting with their mean lines for 3-D classification of potholes are shown in Fig. 5.10. The pothole classification is given in Table 5.3.

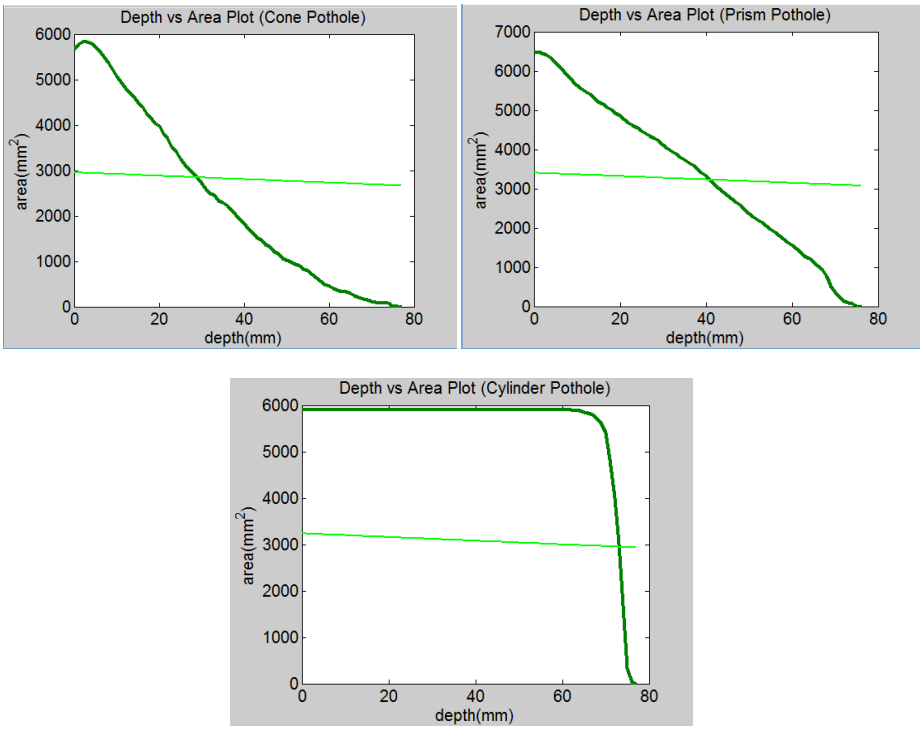

Figure 5.10. Depth Vs Area curves intersecting there mean line for 3-D classification of potholes

Table 5.3. Pothole classification

Pothole name	Eccentricity	Intersection on average line			Classification
		<60%	60% to 80%	>80%	
Hemisphere	.0906		√		Transverse, TTADP
Prism	.9166		√		Longitudinal, TTADP
Pyramid	.2461	√			Transverse, FTADP
Cone	.2766	√			Transverse, FTADP
Cylinder	.1921			√	Transverse, NDP
Cube	.1182			√	Transverse, NDP

5.4. SUMMARY

This chapter details

- A test-rig which is constructed and designed for the purpose of comparison between manual and algorithm based measurement.
- Six artificial potholes of different shapes and dimensions are created in the test-rig.
- The percentage error in depth and volume are calculated and listed.
- Mean Percentage Error (MPE) for Pothole maximum depth is found to be 2.58 %.
- Mean Percentage Error (MPE) for Pothole volume is found to be 5.47 %.
- 2-D classification of potholes, which describe about the outer shape of the pothole.
- A 3-D classification, which provide information about the pothole area change with respect to its depth.

6. PERFORMANCE ANALYSIS

The chapter details Kinect sensor performance under different conditions where potholes are filled with clear water, muddy water and in case of lube oil droppings from vehicles on the road. In rainy conditions potholes are filled with water, moreover sometimes the water in potholes contains certain level of mud in it. Additionally, lube oil droppings on road create a different scenario in the case, where lube oil is floating over the surface of water. Some experiments are done to see the performance of Kinect sensor under these abnormal conditions.

6.1. ERROR INTRODUCED BY ROAD SURFACE ROUGHNESS

A pothole with its binary images at few depths is shown in Fig. 6.1. At initial 15 millimeters, from the top of the pothole, it is observed that the pothole boundary is confused with the surface roughness of the pavement. The corresponding area-depth curve of pothole shown in Fig. 6.1, is shown in Fig. 6.2. It is clear from the area-depth curve that a large error is introduced due to the pavement surface roughness, which should be removed. So, mean rise in depth values is calculated and road surface effected values are replaced by it and initial 15 millimeters as shown in Fig. 6.3.

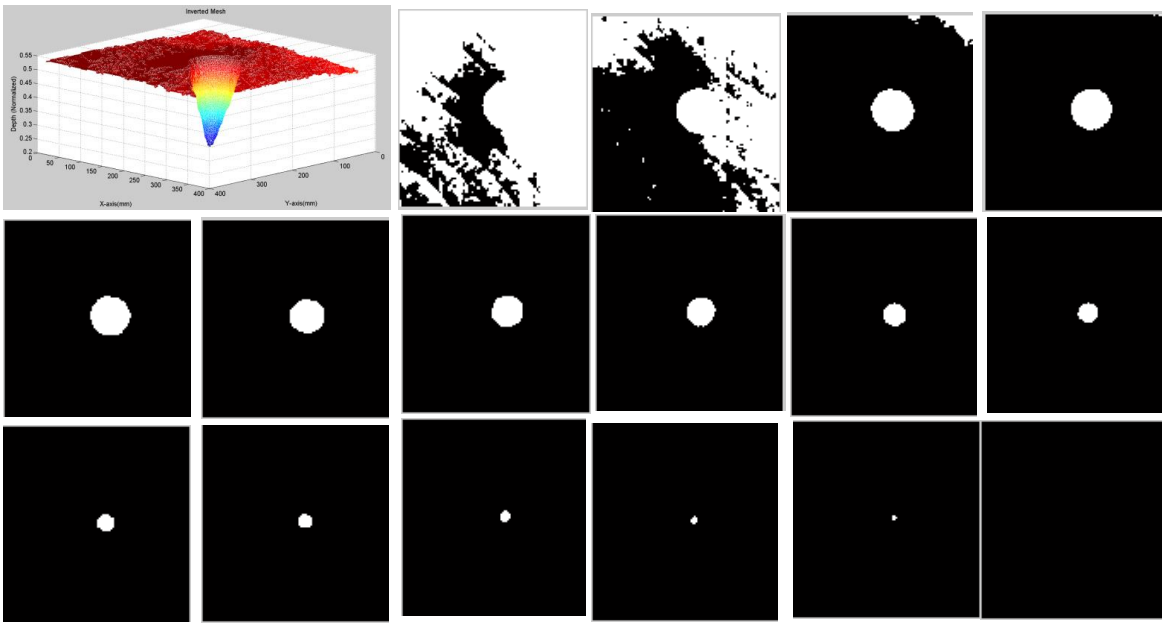

Figure 6.1. Binary Images of Pothole at 1,4,7,10,15,20,25,30,35, 40,45,50,55, 60,70 and 80 millimeters depth respectively

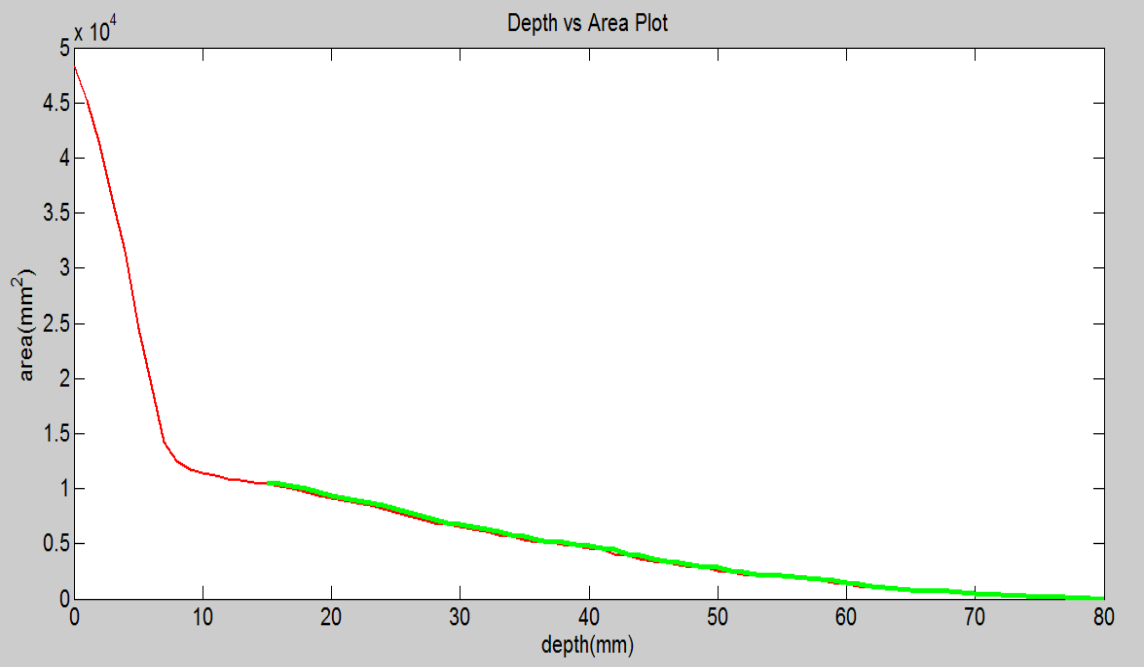

Figure 6.2. Plot of Area decay Vs. Depth (Effected with Surface Roughness)

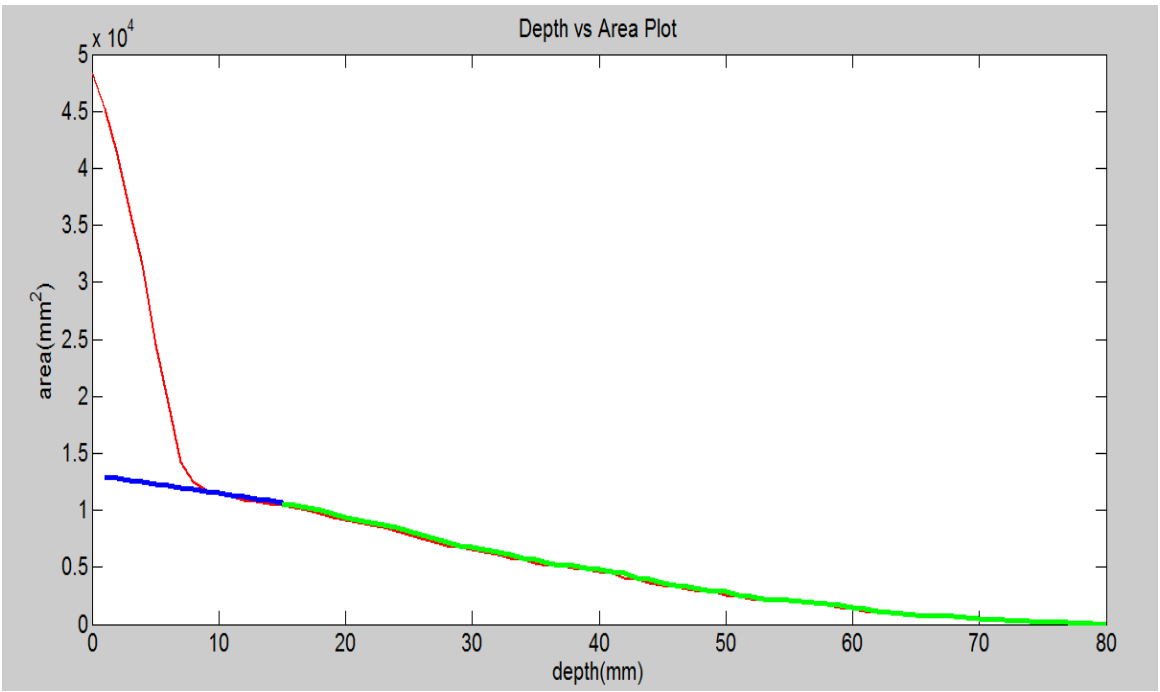

Figure 6.3. Plot of Area decay Vs. Depth (Replacing effected Area with Mean curve rising trend)

6.2. NEGATIVE DEPTH REMOVAL

Negative depths are pebbles, stones, speed breakers or rocks on the road surface, which if not incorporated in the algorithm, will become a cause of severe errors in metrological calculations. When fitted plane is subtracted from tilted image, negative depths will have negative values. Simply converting double data class to unit8 (8 bit unsigned integer) class remove the negative depths by converting each negative value to zero. A pothole with stones around it is shown in Fig. 6.4, to demonstrate the removal of these negative depths.

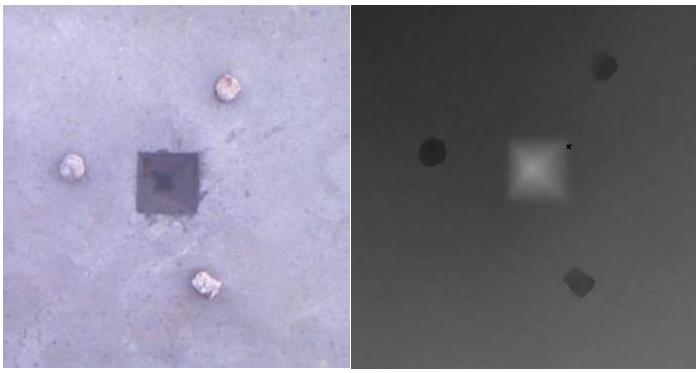

RGB Image Depth Image

Figure 6.4. RGB and depth images of scenario with stones as negative depths around pothole

Mesh with negative depths is shown in Fig. 6.5. Mesh after subtracting fitted plane from tilted image in shown in Fig. 6.6, the negative depths have taken negative values. Converting double to unit8 data type provides mesh with removed negative depths as shown in Fig. 6.7.

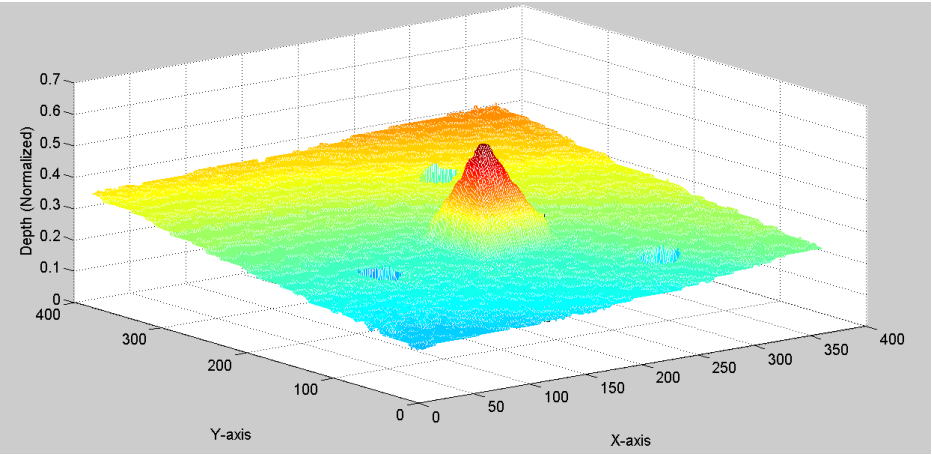

Figure 6.5. Mesh with negative depths visible

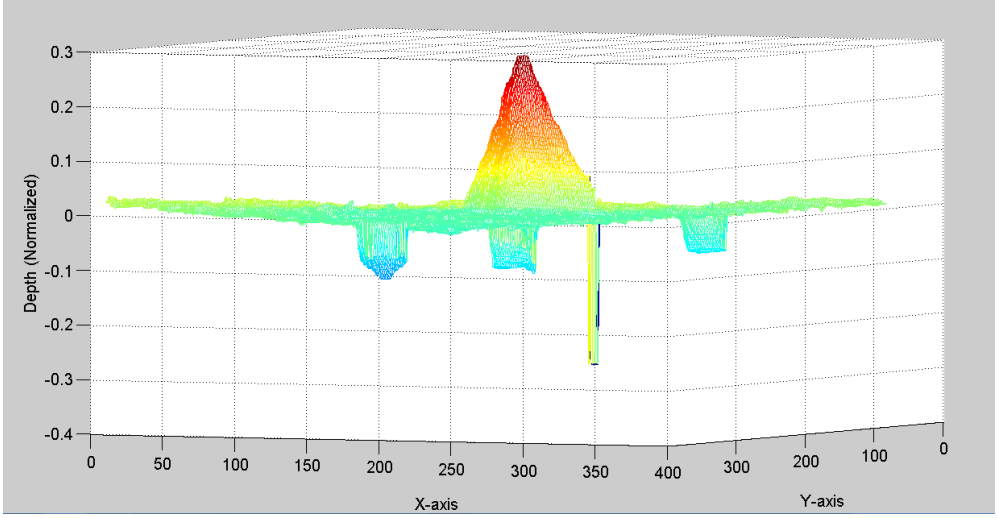

Figure 6.6. Mesh after subtracting fitted plane

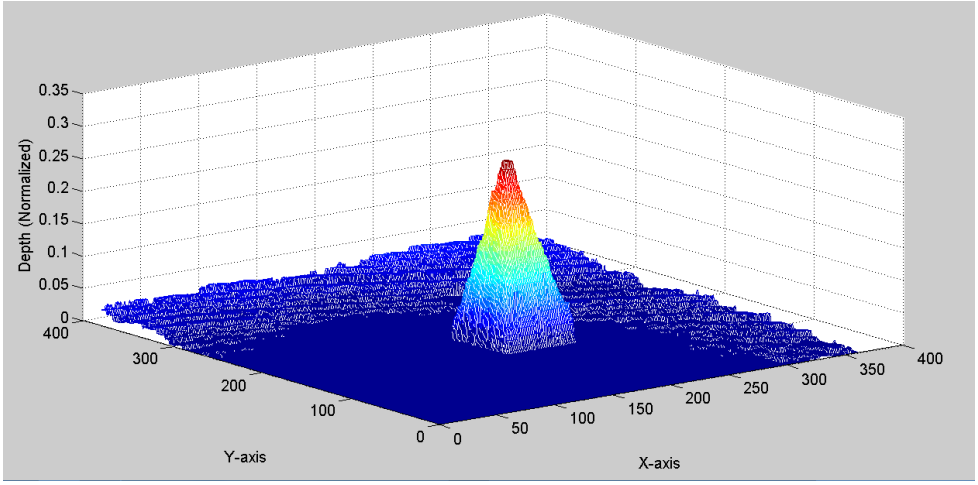

Figure 6.7. Removed negative depths

6.3. RESULTS WITH CLEAR WATER IN POTHOLES

An experiment is performed to check Kinect's performance in the case, where potholes are filled with different percentage of water, by their volume. The test-rig potholes are filled with water at 20, 40, 60, 80 and 100% by their volume and volumetric results are generated. A decrease in volume calculation is observed as the content of water is enhanced in the potholes. The results are listed in table 6.1. The decrease in mesh size of one pothole, when water content is increased in it, is shown in Fig. 6.8.

Table 6.1. Clear Water Experiment

Pothole Name	Actual Volume	20 % Filled		40 % Filled		60 % Filled		80 % Filled		100 % Filled	
		Mean	Error (%)	Mean	Error (%)	Mean	Error (%)	Mean	Error (%)	Mean	Error (%)
Prism	545	566	4	387	-28	516	-5	452	-17	453	-17
Pyramid	340	304	-10	281	-17	298	-12	282	-17	290	-14
Cone	403	297	-26	292	-27	262	-34	234	-41	258	-36
Cylinder	950	877	-8	832	-12	816	-14	736	-22	710	-25
Cube	780	610	-21	692	-11	557	-28	557	-28	574	-26

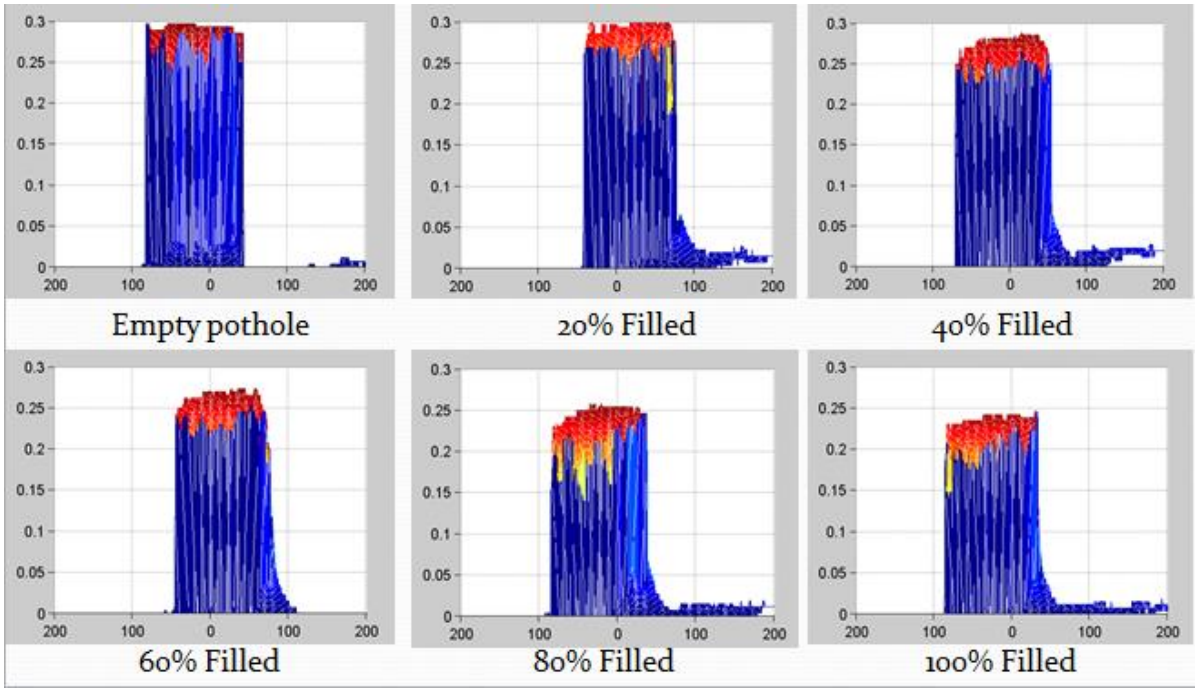

Figure 6.8. Pothole filled with different content of water

6.4. RESULTS WITH MUDDY WATER IN POTHOLES

An experiment is performed to check Kinect's performance in the case, where potholes are filled with muddy water, at different mud content, in a solution of 100 ml. The test-rig potholes are filled with 100 ml solution at mud content of 20000, 40000, 60000, 80000 and 100000 PPM and volumetric results are generated. A random behavior in volume calculation is observed due to random distribution of un-dissolved mud particles. The results are listed in table 6.2. The random mesh results due to dissolved and un-dissolved dust particles are shown in Fig. 6.9. The randomness in error obvious from table 6.2 is caused by two major

facts. When a high level of mud is dissolved in water, then the muddy water behaves like an opaque surface. The infrared rays coming from the sensor IR projector are reflected back from the surface of water and so the volume contained by muddy water cannot be evaluated. Due to which, an error is introduced. Secondly, sometimes the IR rays from the sensor are completely absorbed by dissolved mud particles in muddy water. As these rays do not make their way back to the IR sensor, the depth at those pixel locations is not measured, which in turn creates an error. These two types of error are the main cause of randomness in error as compared to normal conditions when potholes are empty.

Table 6.2. Muddy Water Experiment

Pothole Name	Actual Vol-ume	20,000 PPM		40,000 PPM		60,000 PPM		80,000 PPM		100,000 PPM	
		Mean	Error (%)	Mean	Error (%)	Mean	Error (%)	Mean	Error (%)	Mean	Error (%)
Prism	545	507	-6	255	-53	197	-63	400	-26	149	-72
Pyramid	340	177	-47	255	-25	116	-65	50	-85	108	-68
Cone	403	161	-60	113	-71	162	-66	90	-77	185	-54
Cylinder	950	798	-16	731	-23	773	-18	857	-10	731	-23
Cube	780	653	-16	572	-26	662	-15	492	-37	579	-26

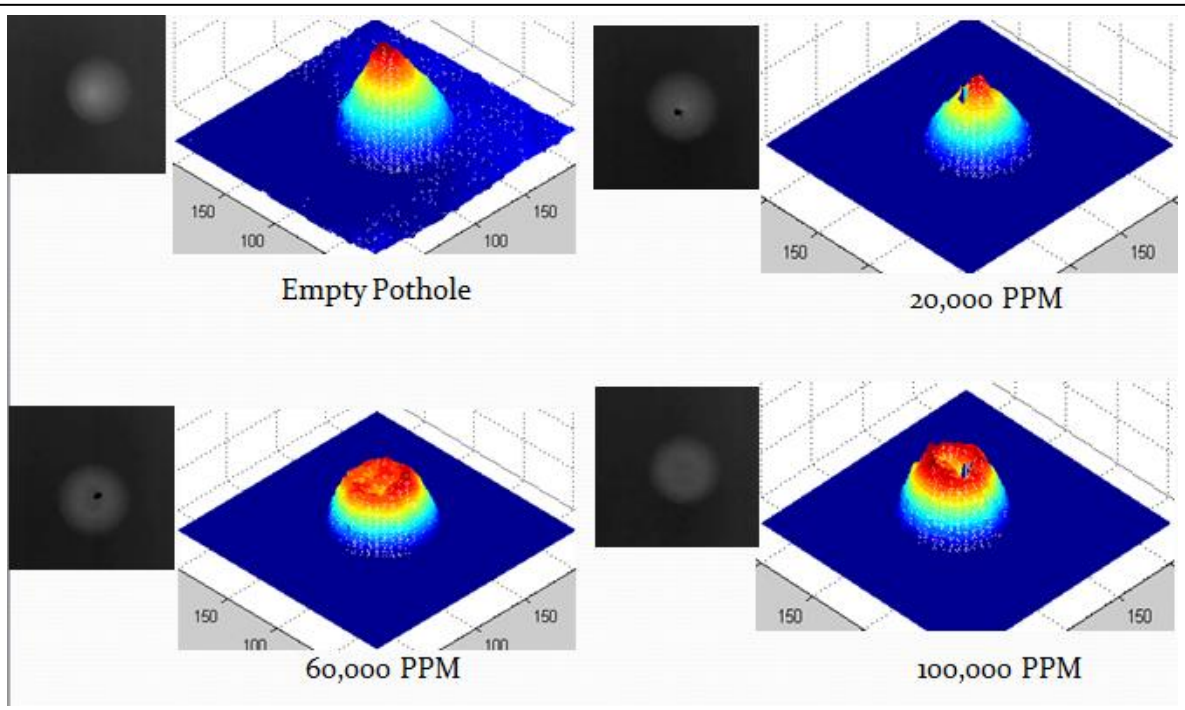

Figure 6.9. Pothole meshes at different PPM of dust in water

6.5. RESULTS WITH LUBE OIL IN POTHOLES

An experiment is performed to check Kinect's performance in the case, where potholes are filled with a solution of lube oil and water, at different lube oil content in the solution of 100 ml. The test-rig potholes are filled with 100 ml of solution at lube oil content of 0.5, 1, 1.5, 2 and 2.5 ml and volumetric results are generated. A random behavior in volume calculation is observed due to random distribution of un-dissolved lube oil on the surface of water. The results are listed in table 6.3. The results of a pothole filled with different solutions in shown in Fig. 6.10. The Kinect sensor is not disturbed by lube oil spillage on pavement under normal conditions but dark low grade black un-dissolved lube oil on the surface of water in the potholes creates a worst condition, where Kinect's IR rays are absorbed by the lube oil content. As a result, depth is not measured by sensors at those specific areas. This result in random error as listed in Table 3 due to random distribution of lube oil on surface of water in the potholes.

Table 6.3. Lube Oil Experiment

Pothole Name	Actual Volume	0.5 ml		1 ml		1.5 ml		2 ml		2.5 ml	
		Mean	Error (%)	Mean	Error (%)	Mean	Error (%)	Mean	Error (%)	Mean	Error (%)
Prism	545	402	-26	136	-75	159	-70	214	-60	238	-56
Pyramid	340	141	-58	19	-94	46	-75	63	-81	68	-80
Cone	403	180	-55	26	-93	171	-57	64	-84	72	-47
Cylinder	950	738	-22	522	-45	650	-31	191	-79	60	-93
Cube	780	639	-18	554	-28	444	-43	44	-94	7	-99

6.6. PIXEL SIZE CALCULATION

Pixel size means physical length of the road surface as measured by a pixel at any given depth is calculated using the law of cosines and the field of view of Kinect. As we know Kinect field of view in both horizontal and vertical directions, which are 58 degrees and 45 degrees respectively, and we also know the Kinect's imaging height i.e. 0.8 meters, from law of cosines we calculate imaging length and width respectively.

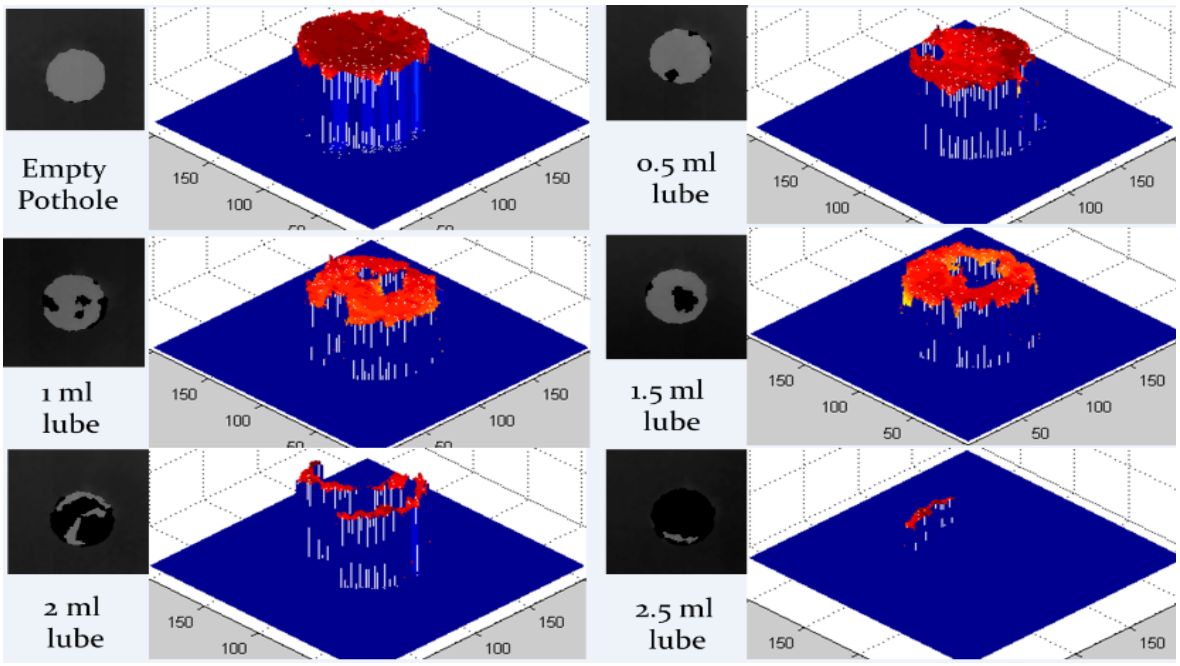

Figure 6.10. Pothole meshes at different content of lube oil on the surface of water

As we also know that depth images resolution is 640x480 pixels, so we divide imaging length and width by 640 and 480 respectively to get pixel length and width respectively. The law of cosines is given in equation 6.1.

$$(I.A)^2 = 2 \text{ x } (I.H)^2\text{-}2 \text{ x } (I.H)^2 \text{ x } cos(A) \qquad [6.1]$$

Where,

I.A : Imaging area

I.H : Imaging height

A : angle of view of Kinect

6.7. RESOLUTION VS. IMAGING HEIGHT

The range of the Kinect sensor is 0.8 to 4 m. Its resolution decreases as the imaging height is increased. The relation between imaging height and pixel size or "physical length of road surface" as measured by a pixel at any given imaging height is drawn in Fig. 6.11, applying "law of cosines" utilizing Matlab. The red and green lines show the increase of length of pixel in Kinect's horizontal and vertical orientation as the Imaging height is increased. The blue line show corresponding physical area of the road as measured by a pixel.

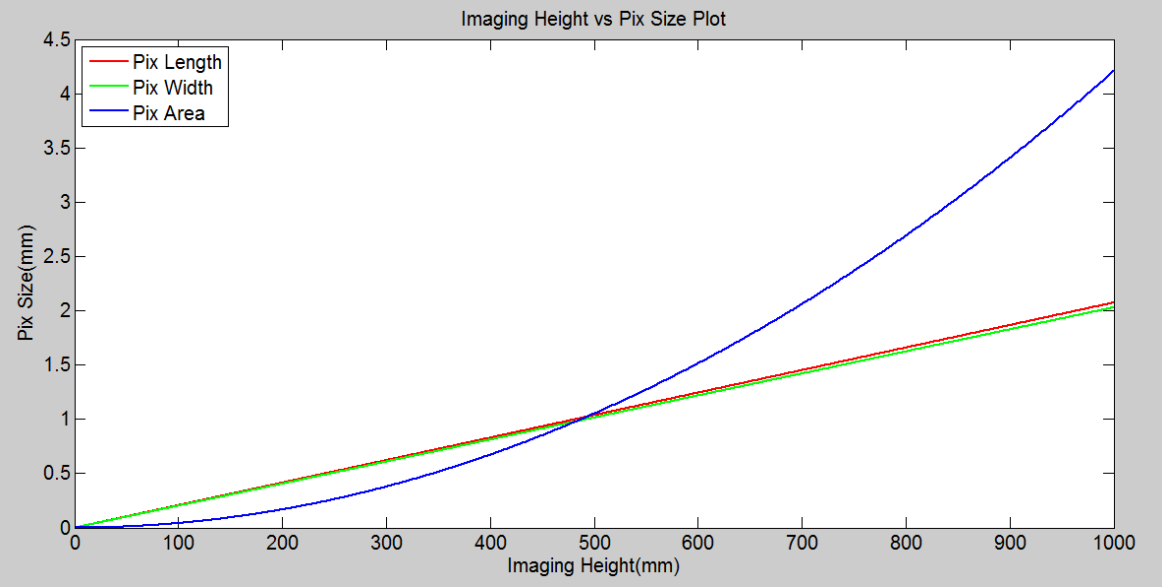

Figure 6.11. Imaging height vs. pixel size

6.8. IMAGING HEIGHT VS. IMAGING LENGTH

The relation between imaging height and imaging length is drawn in Fig. 6.12. Imaging length increases as the height of the sensor is increased. The red and green lines show the increase of imaging length in Kinect's horizontal and vertical orientation as the Imaging height is increased. From Fig. 6.12, "number of sensors to scan certain width of road" can also be calculated from the imaging length at specific imaging height.

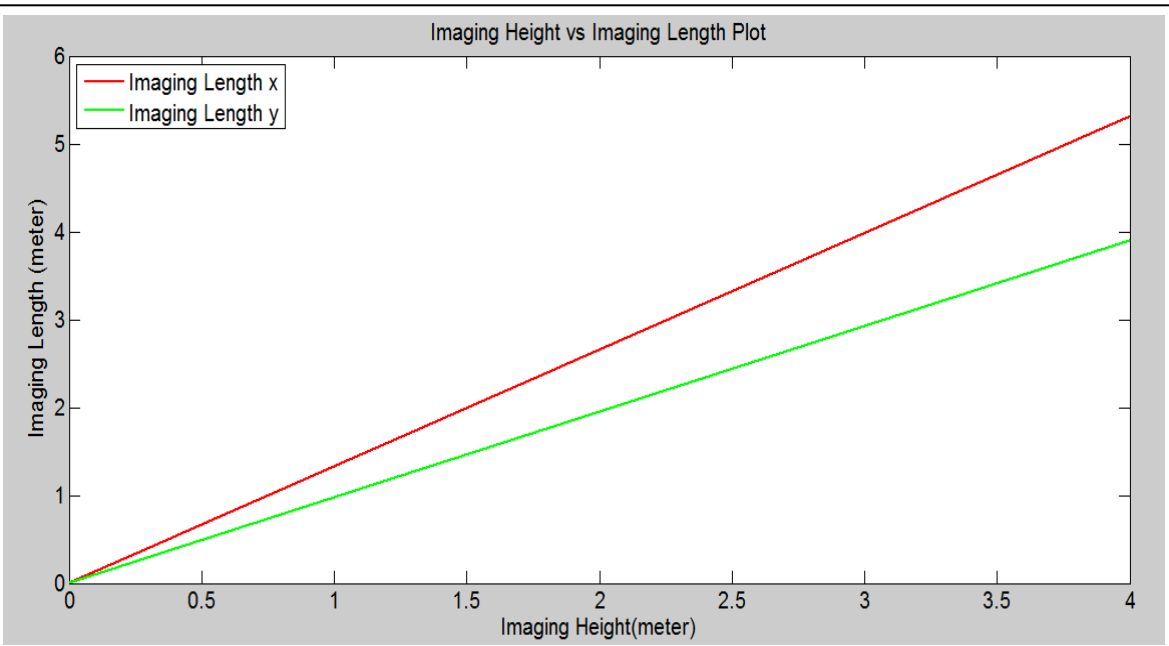

Figure 6.12. Imaging height vs. imaging length

6.9. SUMMARY

This chapter describes that

- The mean rise in depth values is calculated and road surface effected values of area-depth curve are replaced by it and initial 15 millimeters to remove error due to the pavement surface roughness.
- Converting double to unit8 data type provides mesh with removed negative depths.
- A decrease in volume calculation is observed as the content of clear water is enhanced in the potholes.
- The maximum Error is found to be 26, 28, 34, 41 and 36 percent in the case, where potholes are filled with clear water at 20, 40, 60, 80 and 100 percent by their volume respectively.
- A random behavior in volume calculation is observed due to random distribution of un-dissolved mud particles, in the case where there is muddy water in potholes.
- The maximum Error is found to be 60, 71, 66, 85 and 72 percent in the case, where potholes are filled with muddy water at mud content of 20000, 40000, 60000, 80000 and 100000 PPM respectively.
- A random behavior in volume calculation is observed due to random distribution of un-dissolved lube oil on the surface of water.
- The maximum Error is found to be 58, 94, 75, 84 and 99 percent in the case, where potholes are filled with 100 ml of solution at lube oil content of 0.5, 1, 1.5, 2 and 2.5 ml respectively.
- The resolution decreases as the imaging height is increased.

7. CONCLUSION AND FUTURE WORK

7.1. CONCLUSION

The Kinect sensor shows good promise for pavement visualization and metrological analysis of the pavement potholes. Different metrological and geometrical parameters of the potholes have shown to be extracted by analyzing the depth images acquired by this sensor. It provides more detailed information regarding pavement distress as compared to 2-D vision technique. Moreover the camera is capable to working in low or no lighting conditions. Kinect is better than stereo vision in a sense that it requires less computing resources to acquire depth information because the depth measured by IR camera is readily available as it is internally computed within the sensor. It behaves like a smart sensor so external resources are spared. It is also cheaper as compared to lasers setups designed for pavement inspection in equipment and operating cost as laser systems require high power consumption. The sensor is very efficient in finding pothole geometry parameters such as major axis, minor axis, centroid, eccentricity, orientation, perimeter, maximum depth and volume. Maximum Error is found to be 3.8 and 7.9 percent in the case of maximum depth and volume respectively. Potholes can be easily classified based on their 2-D and 3-D geometry. Filling potholes with water create error in volume calculation. A decrease in volume calculation is observed as the water content in pothole in increased. Results with muddy water show limitation of Kinect sensor in finding volume under dense muddy water where infrared light reflects back from surface of muddy water considering it an opaque surface in the case, where dust particles are dissolved in water in high concentration. Also due to un-dissolved dust particles, sometimes the IR rays from the sensor projector are absorbed, and do not make their way back to the IR sensor, in this case sensor is unable to find any distance value, provide zero depth value and a large error is introduced in calculations. When lube oil is spilled on road surface then the sensor is able to find depth information efficiently but lube oil on surface of water in potholes create a worst case scenario where IR rays are absorbed by the lube oil and the sensor reads zero depth at those locations, introducing a large error in volume calculations. Under normal conditions the sensor can be utilized for pavement inspection with considerable accuracy.

7.2. FUTURE WORK

- Future aim includes the development of a robust algorithm in order to stabilize the Kinect images in motion while recording a sequence of depth images during pavement survey. The built-in accelerometer in the sensor can be used to stabilize depth images.
- From different parameters of the pothole like its depth, length, width and orientation, and from its area decay curves, a severity factor can be calculated, which will describe how dangerous is that pothole to the traffic, and subsequently a priority repairing queue of potholes can be generated.
- Based on the present geometry of the pothole, its further decay can be predicted and its repairing priority can be set.
- GPS integration with this pavement survey in real time can be used to locate detected potholes to get ease in locating potholes while repairing.
- Design of Stable Mobile Platform can be another future work to minimize errors introduced by unstable platform and vehicular vibrations.

REFERENCES

[1] J. Eriksson, L. Girod and B. Hull, "The Pothole Patrol Using a Mobile Sensor Network for Road Surface Monitoring," *Proceedings of the 6th international conference on Mobile systems*, applications, and services, 2008.

[2] P. Aksamit and M. Szmechta, "Distributed, mobile, social system for road surface defect detection," *5th International Symposium on Computational Intelligence and Intelligent Informatics*, September 15-17, 2011, Floriana, Malta.

[3] C. Koch and I. Brilakis, "Improving Pothole Recognition through Vision Tracking for Automated Pavement Accessment," *Proceedings of the 18th EG-ICE Workshop on Intelligent Computing in Engineering*, 6-8 July 2011, Twente, Netherlands.

[4] M. I. Rajab, M. H. Alawi and M. A. Saif, "Application of Image Processing to Measure Road Distresses," *WSEAS Transactions On Information Science& Applications*, Issue 1, Volume 5, January 2008.

[5] X. Yao, M. Yao and B. Xu, "Automated Detection and Identification of Area-based Distress in Concrete Pavements," *7th International Conference on Managing Pavement Assets*, 2008.

[6] J. Lin and Y. Liu, "Potholes Detection Based on SVM in the Pavement Distress Image," *Ninth International Symposium on Distributed Computing and Applications to Business*, Engineering and Science, 2010.

[7] E. Salari and X. Yu, "Pavement Distress Detection and Classification Using A Genetic Algorithm," *Applied Imagery Pattern Recognition Workshop (AIPR)*, 2011 IEEE.

[8] H.Youquan, W.Jian, Q.Hanxing, Z. Wei and X. Jianfang, "A Research of Pavement Potholes Detection Based on Three-Dimensional Projection Transformation," *4th International Congress on Image and Signal Processing* , 2011.

[9] E. Salari and G. Bao, "Automated Pavement Distress Inspection basedon 2D and 3D Information," Electro/Information Technology (EIT), *2011 IEEE International Conference on*, 2011.

[10] K. C. P. Wang and W. Gong, "Automated Pavement Distress Survey: A Review and A New Direction," Pavement Evaluation Conference, 21-25, 2002, Roanoke, Virginia.

[11] X. Yu and E. Salari, "Pavement Pothole Detection and Severity Measurement Using Laser Imaging," Electro/Information Technology (EIT), *2011 IEEE International Conference on*, 2011.

[12] N. T. Sy, M. Avila, S. Begot and J. C. Bardet, "Detection of Defects in Road Surface by a Vision System," *Electrotechnical Conference*, 2008. MELECON 2008, The 14th IEEE Mediterranean.

[13] J. Laurent, M. Talbot and M. Doucet, "Road surface inspection using laser scanners adapted for the high precision 3D measurements of large flat surfaces," 3-D Digital Imaging and Modeling, *International Conference on Recent Advances in*, 1997.

[14] S. Cafiso and A. D. Graziano, "Evaluation Of Pavement Surface Distress Using Digital Image Collection And Analysis," *Seventh International Congress on Advances in Civil Engineering*, October 11-13, 2006,Yildiz Technical University, Istanbul, Turkey

[15] E. S. Li, "Physical Optics Models for the Backscatter Response of Road-Surface Faults and Roadside Pebbles at Millimeter-Wave Frequencies," *IEEE Transactions on Antennas And Propagation*, VOL. 51, NO. 10, OCTOBER 2003.

[16] L. Wei, T. F. Fwa and Z. Zhe, "Pavement Roughness Analysis Using Wavelet Theory," *6th International Conference on ManagingPavements*, 2004.

[17] L. Cruz, D. Lucio, L. Velho, "Kinect and RGBD Images: Challenges and Applications," Graphics, Patterns and Images Tutorials (SIBGRAPI-T), 2012 25th SIBGRAPI Conference on.

[18] P. Rakprayoon, M. Ruchanurucks and A. Coundoul, "Kinect-based obstacle detection for manipulator," System Integration (SII), 2011IEEE/SICE International Symposium on Robotics & Control Systems., pp. 68 – 73, 2011.

[19] D. S. O. Correa, D. F. Sciotti, M.G. Prado, D. O. Sales, D. F. Wolf and F. S. Ozone, "Mobile Robots Navigating in Indoor Environments Using Kinect Sensor," Critical Embedded Systems (CBSEC), *Second Brazilian Conference on Computing & Processing (Hardware/Software)*, 2012, pp. 36-41.

[20] R. A. El-laithy, J. Huang and M. Yeh, "Study on the use of Microsoft Kinect for robotics applications," Position Location and Navigation, *Position Location and Navigation Symposium (PLANS)*, 2012 IEEE/ION

[21] D. Joubert, A. Tyatyantsi, J. Mphahlehle and V. Manchidi, "Pothole Tagging System," *4th Robotics and Mechatronics Conference of South Africa (RobMech 2011),* CSIR International Conference Centre, Pretoria, 23-25 November 2011.

[22] M. R. Jahanshahi, F. Jazizadeh, S. F. Masri and B. B. Gerber, "An Unsupervised Approach for Autonomous Pavement Defect Detection and Quantification Using an Inexpensive Depth Sensor," *Journal of Computing in Civil Engineering* (ASCE).

[23] B. Steinauer and D. Kemper, "Condition of the Municipal Road Network," Institut für Straßenwesen Aachen, Final report, 2005.

[24] A. Bianchini, P. Bandini, and D. W. Smith, "Interrater Reliability of Manual Pavement Distress Evaluations," Journal of Transportation Engineering. 136(2), 165–172, 2010.

[25] http://www.southafrica.info/business/economy/development/potholes-190411.htm, "pothole repair programme," (Accessed : 19/09/2013).

[26] American Society of Civil Engineers,"2009 report card for america's infrustructure," 2009.

[27] http://www.tripnet.org, "Key facts about americas road and bridge conditions and federal funding," (Accessed : 11/09/2013).

Completion Certificate

It is to certify that the thesis titled "**Filler Material Estimation for Potholes Using 3D Pavement Images**" submitted by Regn. No. **2011-NUST-MS-PHD-Mts-30**, **Syed Imran Moazzam Shah** of **MS-70 Mechatronics Engineering** is complete in all respects as per the requirements of Main Office, NUST (Exam branch).

Supervisor: _____

Dr. Khurram Kamal

Date: ____ Nov, 2013